Molecular Biotechnology (2021) 63:1192–1222
https://doi.org/10.1007/s12033-021-00374-z

ORIGINAL PAPER

In Silico Design and Immunological Studies of Two Novel Multiepitope DNA-Based Vaccine Candidates Against High-Risk Human Papillomaviruses

Matin Kayyal[1] · Azam Bolhassani[2] · Zahra Noormohammadi[1] · Majid Sadeghizadeh[3]

Received: 15 April 2021 / Accepted: 19 July 2021 / Published online: 25 July 2021

Abstract

Human papillomaviruses (HPV)-16 and 18 are the most prevalent types associated with cervical cancer. HPV L1 and L2 capsid proteins and E7 oncoprotein play crucial roles in HPV-related diseases. Hence, these proteins were proposed as target antigens for preventive and therapeutic vaccines. In this study, two multiepitope DNA-based HPV vaccine candidates were designed using in silico analysis including the immunogenic and conserved epitopes of HPV16/18 L1, L2 and E7 proteins (the L1-L2-E7 fusion DNA), and of heat shock protein 70 (HSP70) linked to the L1-L2-E7 DNA construct (the HSP70-L1-L2-E7 fusion DNA). Next, the expression of the L1-L2-E7 and HSP70-L1-L2-E7 multiepitope DNA constructs was evaluated in a mammalian cell line. Finally, immunological responses and antitumor effects of the DNA constructs were investigated in C57BL/6 mice. Our data indicated high expression rates of the designed multiepitope L1-L2-E7 DNA (~ 56.16%) and HSP70-L1-L2-E7 DNA (~ 80.45%) constructs in vitro. The linkage of HSP70 epitopes to the L1-L2-E7 DNA construct significantly increased the gene expression. Moreover, the HSP70-L1-L2-E7 DNA construct could significantly increase immune responses toward Th1 response and CTL activity, and induce stronger antitumor effects in mouse model. Thus, the designed HSP70-L1-L2-E7 DNA construct represents promising results for development of HPV DNA vaccine candidates.

Keywords Human papillomavirus · Early protein · Late protein · Immunoinformatics tools · Multiepitope DNA vaccine

Introduction

Infectious agents are responsible for 20–25% of all cancer cases in the world [1]. Among them, about 15% of human cancers were related to viral infections [2, 3]. For example, human papillomavirus (HPV) caused ~ 30% of all infectious agents-related cancers, and was associated with more than 95% of cervical carcinomas [4–6]. The genome of HPV is divided into two main regions encoding early (E) and late (L) proteins. The early proteins regulate the viral DNA replication in the basal layer of epithelial cells, and the late proteins make viral capsid [7–9]. Among early proteins, E6 and E7 oncoproteins are required for the initiation of HPV-associated malignancies and are expressed in transformed cells. Therefore, HPV E6 and E7 oncoproteins serve as ideal targets for therapeutic HPV vaccines [10].

Among more than 200 recognized HPV genotypes, two high-risk HPV types such as HPV16 and HPV18 have been recognized as the most prevalent types related to nearly 70% of cervical cancers and precancerous cervical lesions [11, 12]. Hence, considerable efforts have been made to control HPV-induced diseases using prophylactic or therapeutic approaches [13, 14]. Up to now, three prophylactic HPV vaccines were FDA-approved based on viral like particles (VLPs) composed of L1 protein including Cervarix (bivalent HPV16/18 vaccine), Gardasil (quadrivalent HPV16/18/6/11 vaccine), and Gardasil-9 (nonavalent HPV16/18/31/33/45/52/58/30/40 vaccine) [15]. Although, these vaccines were effective only in subjects who were not previously exposed to HPV, but none of them did not show therapeutic effects on the established HPV infection and associated cancers. Furthermore, their high cost is a major

✉ Azam Bolhassani
azam.bolhassani@yahoo.com; A_bolhasani@pasteur.ac.ir

1 Department of Biology, Science and Research Branch, Islamic Azad University, Tehran, Iran

2 Department of Hepatitis and AIDS, Pasteur Institute of Iran, Tehran, Iran

3 Department of Genetics, Faculty of Biological Sciences, Tarbiat Modares University, Tehran, Iran

problem in low-income countries [16, 17]. Therefore, development of strong and potent therapeutic vaccine is vital, as well.

Various types of therapeutic vaccines including live bacterial/viral vectors-, RNA/DNA-, protein/peptide- and cell-based vaccines have been tested to treat the HPV-associated diseases [18–20]. For example, some vaccines have passed clinical trials including SGN-00101 protein vaccine (composed of heat shock protein fused to HPV16 E7), ZYC-101a DNA vaccine (composed of HPV16/18 E6 and E7), HPV16 L1-E7 chimeric VLP, TA-HPV (composed of recombinant vaccinia virus expressing E6 and E7), TA-CIN protein vaccine (composed of fusion E6-E7-L2 protein), and PC10VAC01 (composed of HPV16 E7 + adenylate cyclase) [21]. However, each vaccination approach indicated some benefits and limitations [18]. Thus, it is crucial to find the potent and safe strategies in developing therapeutic vaccine and enhancing their immunogenicity [22, 23].

Some studies reported the benefits of heat shock proteins (HSPs) as an adjuvant to increase the antitumor potency of vaccines. HSPs effectively stimulate both innate and adaptive immunity [24, 25]. Among various types of HSPs, HSP70 is a promising molecule because of its adjuvant activity to increase the antigen-specific immunity [24–29]. As known, immunoinformatics tools may assist scientists to predict high immunogenic and conserved epitopes, which induce B- or T-cell responses against HPV infection [20, 30–35]. Moreover, linkage of antigens to HSPs provided a promising strategy to increase the efficiency of vaccine candidates [29, 36].

In current study, in silico approaches were used to design the multiepitope L1-L2-E7, and HSP70-L1-L2-E7 constructs as novel and potent vaccine candidates. The E7 protein was used alone or combined with other HPV proteins especially E6 protein for development of therapeutic clinical trials [21]. Herein, we used E7 protein along with L1 and L2 proteins for design of vaccine constructs. For in vitro assay, the expression of both multiepitope DNA constructs was studied in a mammalian cell line. Finally, the immunological and antitumor effects of both DNA constructs were investigated in C57BL/6 mice.

Materials and Methods

Materials

The restriction enzymes and DNA or protein ladder were purchased from Fermentas Company. DNA extraction kits were prepared from Qiagen Company. The cell culture medium, serum, antibiotic were purchased from Gibco or Biosera Company. The cell lines were provided from the cell bank at Pasteur Institute of Iran. The conjugated antibodies, cytokine and granzyme B assay kits were purchased from Sigma, Mabtech and eBioscience Company, respectively.

Immunoinformatics Analyses

Protein Sequences

The reference protein sequence of heat shock 70 kDa protein 1A (HspA1A; NP_005336.3) was obtained from the National Center for Biotechnology Information Database (NCBI) (http://www.ncbi.nlm.nih.gov/). The reference HPV16/18 L1, L2, E7 protein sequences were previously determined from NCBI and UniProtKB/Swiss-Prot database, and used for bioinformatics analyses by our group [20, 33, 34].

Plan of the Study

In order to determine the potential $CD8^+$ and $CD4^+$ T-cell epitopes, a two-step plan was designed (Figs. 1 and 2). Briefly, the first step included (a) Epitope prediction bound to MHC-I or MHC-II, (b) TAP transport/proteasomal cleavage analysis, (c) Immunogenicity, allergenicity and toxicity analyses, (d) Prediction of cytokine induction, (e) Population coverage, and (f) Protein-peptide docking analyses (Fig. 1). This step was previously performed for epitope prediction of HPV 16 & 18 L1, L2 and E7 proteins [20, 33, 34]. Herein, we determined the immunogenic and conserved epitopes of HSP70. In the second step, two multiepitope peptide constructs were designed and examined for physicochemical characteristics, protein solubility, B-cell epitope prediction, secondary and 3D structure modeling, refinement of 3D structure, validation of the refined 3D structure, and molecular docking between toll-like receptors and novel constructs (Fig. 2).

HLA Allele Frequency

The frequency of HLA supertypes and alleles was determined from allele frequency net database (AFND) (http://www.allelefrequencies.net/).

T-Cell Epitope Prediction

Determination of T-cell immunodominant epitopes was known as the most critical step for design of a multiepitope-based vaccine candidate using immune-informatics tools [37, 38]. Herein, the design of the multiepitope construct harboring HLA-class I restricted cytotoxic T lymphocyte (CTL) epitopes and also HLA-class II restricted helper T lymphocyte (HTL) epitopes was performed as follows.

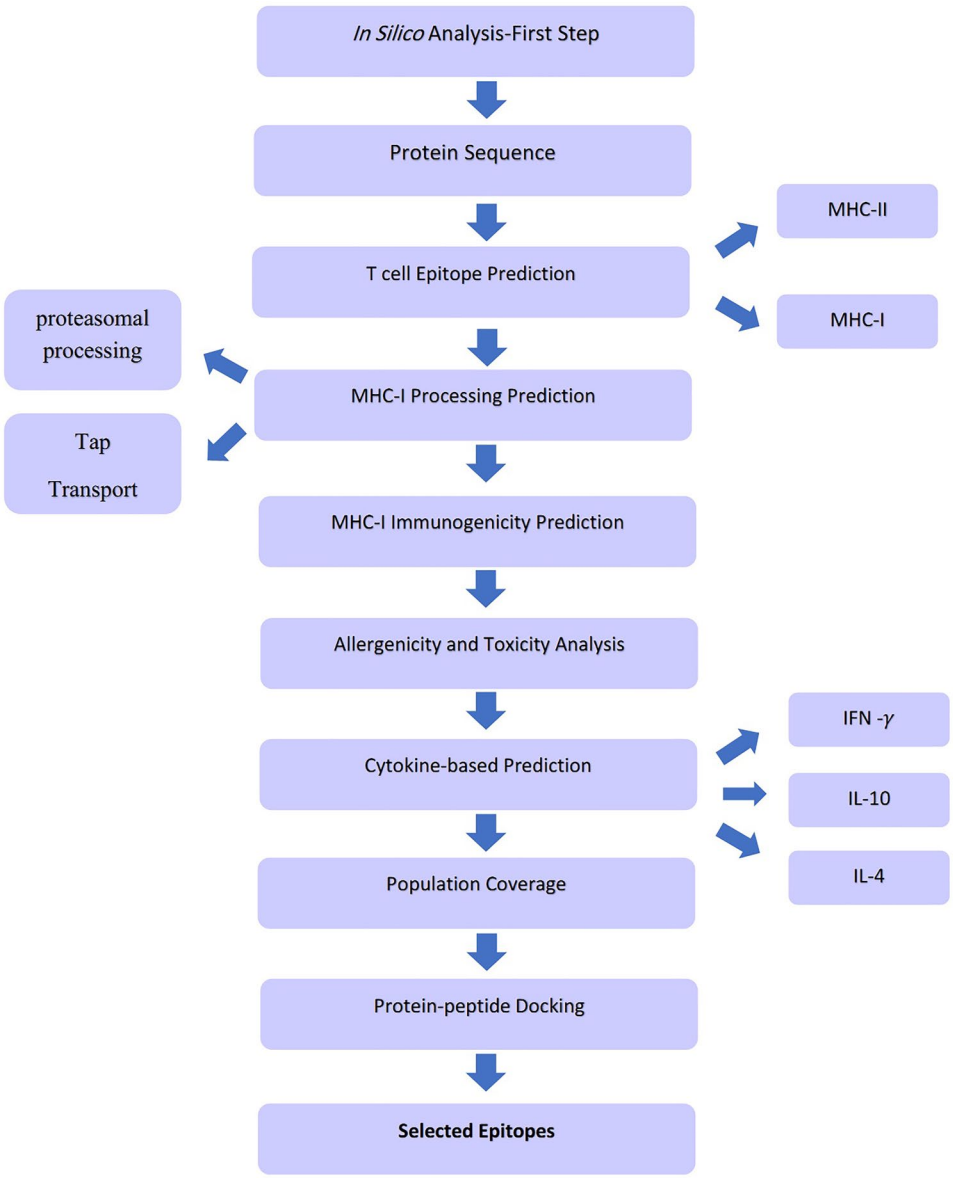

Fig. 1 The first step of in silico analysis

MHC-I Binding Prediction

Binding of MHC class I molecules to epitopes is followed by antigen presentation to CTLs. Herein, IEDB MHC-I prediction (http://tools.iedb.org/mhci/) and NetMHCpan4.1 (http://www.cbs.dtu.dk/services/NetMHCpan/) web servers were applied to predict the binding of peptides (8–11 residues) to MHC class I molecules (default thresholds: 0.5% and 2% for strong and weak binders, respectively) [39]. For prediction of T-cell epitopes of HSP70 bound to human and mouse MHC alleles, IEDB MHC-I prediction tool (IEDB recommended method) was applied, as well. Predictions were performed against H2-Db, H2-Dd, H2-Kb, H2-Kd, H2-Kk, H2-Ld, H2-Qa1 and H2-Qa2 MHC-I mouse alleles.

MHC-II Binding Prediction

Binding of MHC class II molecules to epitopes is critical for the HTL activation [40]. IEDB MHC-II binding prediction tool (http://tools.iedb.org/mhcii/; IEDB recommended method) and NetMHCIIpan 4.0 web server (http://www.cbs.dtu.dk/services/NetMHCIIpan; default thresholds: 2% and 10% for strong and weak binders, respectively) were applied to predict the binding of peptides to MHC-II molecules.

TAP Transport/Proteasomal Cleavage Analysis

The best ranked peptides obtained from IEDB, NetMHCpan4.1, and NetMHCIIpan databases were employed in transporter associated with antigen presentation (TAP),

Fig. 2 The second step of in silico analysis

and proteasomal cleavage analyses. Herein, IEDB tool (http://tools.iedb.org/processing/) and NetCTL1.2 server (http://www.cbs.dtu.dk/services/NetCTL/) were utilized to predict antigen processing in MHC-I presentation pathway. The higher TAP score shows the higher transport rate [41, 42].

MHC-I Immunogenicity Prediction

The IEDB web server (http://tools.iedb.org/immunogenicity/) [43] was applied to determine the MHC-I immunogenicity of the predicted epitopes.

Allergenicity and Toxicity Analyses

An efficient, potent and safe vaccine candidate is not allergic. Herein, the allergenicity and toxicity of the selected epitopes were analyzed by AlgPred server (https://webs.iiitd.edu.in/raghava/algpred/) [44] and ToxinPred web server (https://webs.iiitd.edu.in/raghava/toxinpred/) [45], respectively.

Cytokine Induction-Based Prediction

The chosen epitopes were submitted to evaluate whether they can stimulate Interleukine-10 (IL-10), Interleukine-4 (IL-4), and IFN-gamma using (https://webs.iiitd.edu.in/raghava/il10pred/), (https://webs.iiitd.edu.in/raghava/il4pred/), and (https://webs.iiitd.edu.in/raghava/ifnepitope/) web servers, respectively [46–48].

Population Coverage

Selection of the multiple peptides with different HLA binding specificities will increase the population coverage targeted by peptide-based vaccines [49]. Population coverage for each epitope and its binding to HLA alleles in various geographic areas were analyzed by IEDB population coverage tool (http://tools.iedb.org/population/).

MHC-Peptide Docking

The peptide-protein (e.g., peptide-MHC) interaction is the major goal of computational docking [50]. For prediction of 3D MHC-peptide complex structures, both human and mouse MHC alleles were considered using GalaxyPepDock server (http://galaxy.seoklab.org/cgi-bin/submit.cgi?type=PEPDOCK) based on interaction similarity and energy optimization [51]. The RCSB PDB server (https://www.rcsb.org/) was used to access the available PDB files of HLA alleles.

Construct Design

For design of the multiepitope peptide constructs, immunoinformatics tools were utilized to select novel immunodominant T-cell epitopes. The selected T-cell epitopes of HPV16/18 L1, L2 & E7 proteins [20, 33, 34] were used to design a novel construct fused by AAY linker (the L1-L2-E7 fusion multiepitope peptide construct; Fig. 3A). In addition, the immunodominant T-cell epitopes of HSP70 were linked to the L1-L2-E7 construct for design of the second multiepitope peptide construct (the HSP70-L1-L2-E7 multiepitope construct; Fig. 3B). The HSP70 epitopes as an immune stimulating agent can enhance the immunogenicity of vaccine construct.

B-Cell Epitope Prediction

An effective multiepitope-based vaccine candidate should possess a favorite secondary structure for induction of the peptide-specific humoral response, as well [52]. Thus, both constructs were applied to predict B-cell epitopes using IEDB Bepipred Linear Epitope Prediction (http://tools.iedb.org/bcell/) [53].

Physicochemical Properties

Various physicochemical properties and the solubility of two constructs were predicted by ProtParam server tools

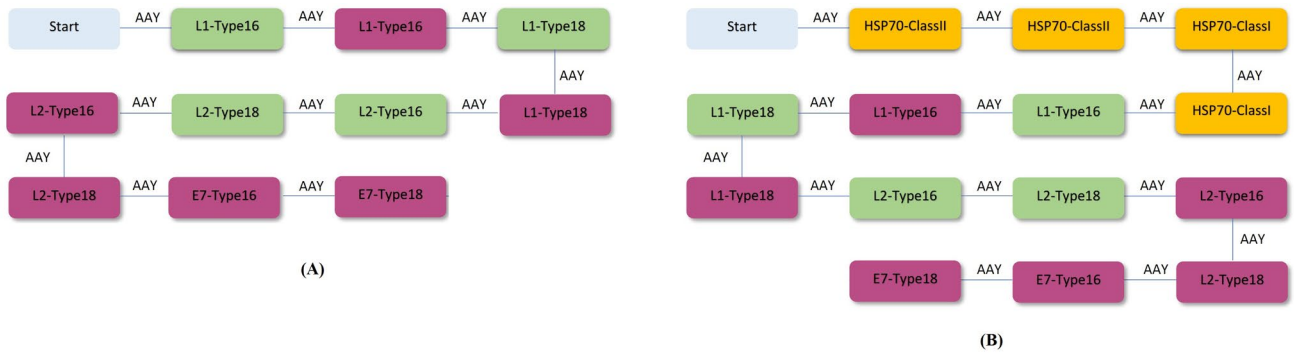

Fig. 3 Schematic diagram of the designed L1-L2-E7 (**A**) and HSP70-L1-L2-E7 (**B**) multiepitope peptide constructs after in silico studies: pink box: CTL epitopes, green box: HTL epitopes, and the alanine-alanine–tyrosine (AAY) peptide as a linker

[54] and protein-sol (https://protein-sol.manchester.ac.uk/) web server, respectively.

Modeling the Secondary Structure

The secondary structures of both constructs were predicted by Predict Secondary Structure (PSIPRED) (http://bioinf.cs.ucl.ac.uk/psipred/) and RaptorX (http://raptorx.uchicago.edu/StructurePropertyPred/predict/) servers. RaptorX Property web server predicts the secondary structure using DeepCNF machine learning model [55].

Modeling, Refinement and Validation of 3D Structures

The tertiary structures of both constructs were predicted by Iterative Threading ASSEmbly Refinement (I-TASSER) server (https://zhanglab.ccmb.med.umich.edu/I-TASSER/) [56]. Then, the refinement of Top 3D structure model determined from I-TASSER was done using GalaxyRefine Server (http://galaxy.seoklab.org/cgi-bin/submit.cgi?type=REFINE) based on molecular dynamics simulation [57, 58]. Finally, validation and selection of the best models of a refined structure were analyzed by ERRAT server (https://servicesn.mbi.ucla.edu/ERRAT/) [59].

Molecular Docking Between the Multiepitope Constructs and Toll-Like Receptors

Molecular docking between the multiepitope peptide constructs and various toll-like receptors (TLRs) was done to predict the possible binding orientation of the multiepitope constructs using ClusPro 2.0 (https://cluspro.bu.edu) [60]. For protein–protein docking, the final refined tertiary structures of the designed vaccine constructs were submitted as ligands [61, 62]. Additionally, the PDB files of TLRs were received from RCSB at https://www.rcsb.org.

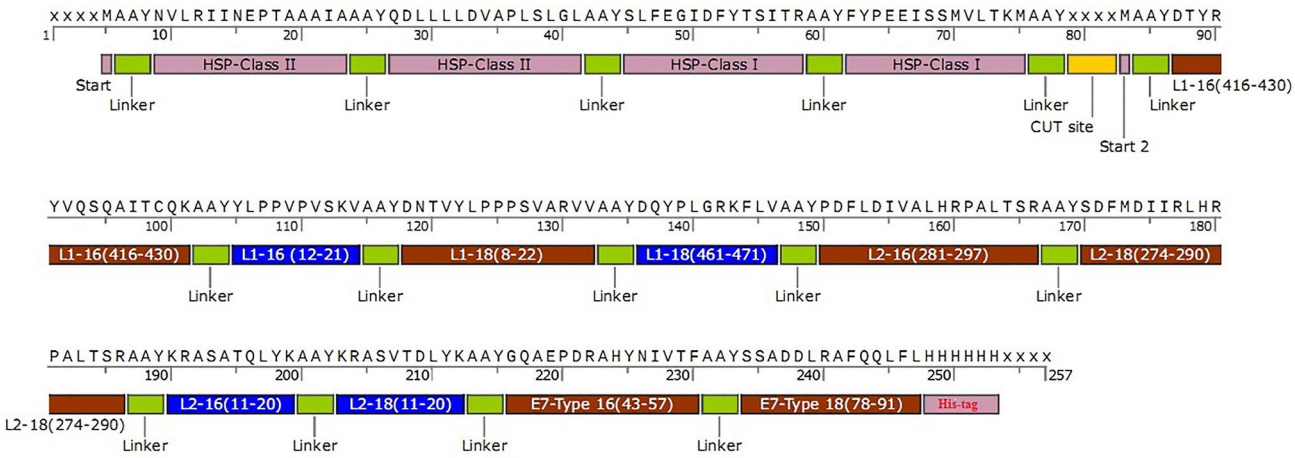

Fig. 4 The HSP70-L1-L2-E7 multiepitope peptide construct: this construct was reversely translated to DNA for in vitro and in vivo studies

In Vitro Analysis

Preparation of the HSP70-L1-L2-E7 DNA Fusion Construct

At first, a general multiepitope peptide construct was designed as shown in Fig. 4. Then, the nucleotide sequence of HSP70-L1-L2-E7 was retrieved by amino acid reverse translation tool (http://www.bioinformatics.org/sms2/rev_trans.html), and the restriction enzyme sites were determined for cloning process. Next, the HSP70-L1-L2-E7 DNA construct was synthesized in pUC57 cloning vector by Bio Magic Gene Company. After that, the L1-L2-E7 and HSP70-L1-L2-E7 genes were subcloned into the *Bgl*II/*Hind*III and *Xho*I/*Hind*III cloning sites of the pEGFP-N1 eukaryotic expression vector, respectively for in vitro studies. In general, the cloning step included digestion of vector and the target gene with the restriction enzymes, gel extraction of the linearized vector and the insert, ligation of the insert and vector by T4 DNA ligase (Fermentas), transformation of the ligation product in *E. coli* DH5α strain, and extraction and confirmation of the recombinant plasmid. Moreover, the L1-L2-E7 and HSP70-L1-L2-E7 genes were subcloned into the *Eco*RI/*Hind*III and *Bam*HI/*Hind*III cloning sites of the pcDNA3.1 (-) eukaryotic expression vector (cytomegalovirus "CMV" promoter), respectively for in vivo studies. Finally, the recombinant endotoxin-free plasmids (i.e., pEGFP-L1-L2-E7, pEGFP-HSP70-L1-L2-E7, pcDNA-L1-L2-E7, and pcDNA-HSP70-L1-L2-E7) were prepared using a Maxi-Kit DNA extraction (Qiagen). Their concentration and purity were revealed by NanoDrop spectrophotometry.

In Vitro Expression of the L1-L2-E7 and HSP70-L1-L2-E7 DNA Constructs in Mammalian Cells

Human embryonic kidney 293T (HEK-293T) cells were cultured in RPMI 1640 medium (Gibco), supplemented with 10% FBS (Fetal Bovine Serum; Biosera, France), 1% Penstrep (Sigma, Germany) at 37 °C and 5% CO_2 in a 24-well plate. When the confluency of the cells reached approximately 80%, the cells were transfected with the TurboFect-plasmid DNA complexes. Herein, 2 µL of TurboFect (Termo Scientifc) and 1 µg of pEGFP-L1-L2-E7, pEGFP-HSP70-L1-L2-E7 or pEGFP-N1 (as a positive control) were mixed and incubated for 20 min at room temperature to form the TurboFect-plasmid DNA complexes. The expression of DNA constructs was analyzed at 48 h after transfection using flow cytometry, fluorescent microscopy, and Western blotting. In Western blotting, the anti-GFP polyclonal antibody (1:5000 v/v; Abcam), and 3,3′-diaminobenzidine (DAB, Sigma) substrate were used to recognize the expressed proteins, and detect the immunoreactive protein bands, respectively.

In Vivo Studies

The Synthesis of Peptide Constructs

For immunological assay, two multiepitope peptide constructs (L1-L2-E7, and HSP70-L1-L2-E7, Fig. 3) were synthesized by BioMatik Company.

Immunization of Mice

Four groups of eight female C57BL/6 mice (maintained at Pasteur Institute of Iran under specific pathogen-free conditions) were injected on days 0, 14, and 28 with the plasmid DNA (pcDNA-L1-L2-E7 or pcDNA-HSP70-L1-L2-E7: G1 or G2; 50 µg) subcutaneously at the right footpad (Table 1). The control groups (G3 and G4) were injected with pcDNA3.1 and PBS, respectively. The animal experimental procedures were approved by Animal Care and Use Committee of Islamic Azad University-Science and Research Branch, and performed according to the Animal Experimentation Regulations of Islamic Azad University for scientific purposes (Ethics code: IR.IAU.SRB.REC.1398.208; Approval date: 2020-02-22).

Monitoring Tumor Growth

For in vivo preventive test, vaccinated mice with different regimens were subcutaneously challenged in the right flank with 1×10^5 HPV16-expressing C3 tumor cells, 3 weeks after the third injection. Tumor cell line C3 was generated by transfection of mouse embryonic cells with the complete HPV genome and maintained as previously described [63]. Tumor growth and the percentage of tumor-free mice were assessed twice a week by palpation for 65 days after C3 challenge. At each time point, tumor volume was calculated using the formula: $V = (a^2b)/2$ (a: width, b: length).

Table 1 Mice immunization program

Groups	First injection (Prime: day 0)	Second injection (Booster 1: day 14)	Third injection (Booster 2: day 28)
G1	pcDNA-L1-L2-E7	pcDNA-L1-L2-E7	pcDNA-L1-L2-E7
G2	pcDNA-HSP70-L1-L2-E7	pcDNA-HSP70-L1-L2-E7	pcDNA-HSP70-L1-L2-E7
G3 (control)	pcDNA3.1 (empty vector)	pcDNA3.1 (empty vector)	pcDNA3.1 (empty vector)
G4 (control)	PBS	PBS	PBS

Antibody Assay

The mice sera were prepared from each group 3 weeks after the third injection. The levels of goat anti-mouse immunoglobulin G1 (IgG1), IgG2a and total IgG antibodies (1:10,000 *v/v*, Sigma) were assessed in the pooled sera of each group (1:100 *v/v*) using indirect ELISA. The coated antigens were the HSP70-L1-L2-E7, and L1-L2-E7 synthetic peptides (5 µg/mL).

Cytokine Assay

Three weeks after the last injection, the red blood cell-depleted pooled splenocytes (2×10^6 cells/mL) of three mice from each group were cultured in 48-well plates for 72 h in the presence of 5 µg/mL of the L1-L2-E7 or HSP70-L1-L2-E7 peptides, negative control (RPMI 5%), and positive control (Concanavalin A: 5 µg/mL). The secretion of IFN-γ, IL-4 and IL-10 was assessed in the supernatants using the sandwich ELISA kit (Mabtech Swedish Biotech Co.). The results were shown as mean ± SD for each group.

Granzyme B Assay (In Vitro CTL Activity)

The P815 target cells (T: 2×10^4 cells/well) were incubated with the L1-L2-E7 or HSP70-L1-L2-E7 peptides (~30 µg/mL) for 24 h. Then, the effector cells (E: the red blood cell-depleted pooled splenocytes) were added to the target cells at T/E ratio of 1/100, and incubated for 6 h. Finally, the concentration of Granzyme B (GrB) was assessed in the supernatants using ELISA (eBioscience kit).

Therapeutic Effects

For therapeutic tests of the established C3 tumors, four groups of five female C57BL/6 mice (similar to Table 1) were considered. Briefly, five mice in each group were subcutaneously injected with 1×10^5 C3 tumor cells, and then 1 week after tumor challenge, mice received various regimens (Table 1, the dose of DNA constructs: 50 µg) three times with a 2-week interval. Finally, tumor growth was detected two times a week for 65 days.

Statistical Analysis

Statistical analysis was done by Prism 7.0 software (GraphPad) using one-way ANOVA and Student's *t*-test. The percentage of tumor-free mice (or survival rate) was determined by the log-rank test. The $p\text{-value} < 0.05$ was statistically considered significant. The experiments were independently performed twice.

Results

In Silico Studies

T-Cell Epitope Prediction

T-cell epitope prediction for the HPV16/18 L1, L2 and E7 proteins was previously done by our group [20, 33, 34]. In this study, the best epitopes were used to design of a fusion construct (L1-L2-E7) for in silico, in vitro and in vivo analyses. Moreover, HSP70 (HspA1A: NP_005336.3) protein sequence was analyzed to identify the most putative immunogenic and conserved regions. The peptides derived from HSP70 were selected based on the strongest binding affinity to human and mouse MHC class I and II alleles. The predicted MHC-I and MHC-II epitopes are listed in Tables 2 and 3.

TAP Transport/Proteasomal Cleavage

TAP transport efficiency and proteasomal cleavage scores were previously determined for L1, L2 and E7 proteins [20, 33, 34]. Herein, HSP70 ^{113}FYPEEISSMVLTKM^{126} and ^{285}SLFEGIDFYTSITR^{298} epitopes had the highest epitope identification scores as shown in Table 4.

Immunogenicity, Toxicity and Allergenicity Analyses

Immunogenicity, toxicity and allergenicity for the L1, L2 and E7 epitopes of HPV types 16 and 18 were analyzed in our previous studies [20, 33, 34]. Herein, these analyses were performed for the selected Hsp70 epitopes as shown in Table 5. As observed, these peptides were non-allergen and non-toxic.

Cytokine Analysis

The MHC class II binding epitopes of HPV16/18 L1, L2 and E7 proteins as well as HSP70 were analyzed for the possible induction of IFN-γ, IL-10 and IL-4 cytokines. The higher rates showed more potent epitopes for inducing cytokines as shown in Table 6. For instance, all candidate epitopes of HPV16/18 L1, L2 and E7 proteins and HSP70 induced IFN-γ cytokine.

Population Coverage Analysis

In our previous study, population coverage was calculated for the selected HPV16/18 L1, L2 and E7 epitopes [20, 33, 34]. Herein, the highest population coverage was determined for HSP70 epitopes in different area. The rates were

Table 2 The selected CTL epitopes of HSP70 protein based on binding affinity

Epitope sequence	Position	Human alleles			Mouse alleles	
		Top alleles	IEDB average rank	NetMHCIpan average rank	Top alleles	IEDB average rank
FYPEEISSMVLTKM	113–126	HLA-A2402	2.20684	1.84686	H2-Db	2.0006
		HLA-A2601			H2-Dd	
		HLA-B1402			H2-Kb	
		HLA-B5101			H2-Kd	
		HLA-B0702			H2-Kk	
		HLA-B3901			H2-Ld	
		HLA-B4001			H2-Qa1	
		HLA-B3501			H2-Qa2	
		HLA-B5101				
		HLA-B*55:01				
		HLA-B*41:01				
		HLA-B*50:01				
		HLA-B*49:01				
		HLA-A1101				
		HLA-A6801				
		HLA-B1801				
		HLA-B4402				
		HLA-A0301				
		HLA-B5801				
SLFEGIDFYTSITR	285–298	HLA-A0101	2.33934	2.1318	H2-Db	2.31923
		HLA-A0301			H2-Dd	
		HLA-A2601			H2-Kb	
		HLA-B1501			H2-Kd	
		HLA-A1101			H2-Kk	
		HLA-B3501			H2-Ld	
		HLA-B*13:01			H2-Qa1	
		HLA-A0201			H2-Qa2	
		HLA-B4001				
		HLA-B1801				
		HLA-B4402				
		HLA-B*41:01				
		HLA-B*50:01				
		HLA-B*52:01				
		HLA-B*49:01				
		HLA-B*55:01				
		HLA-A6801				

88.39% and 81.19% for CTL epitopes of $HSP70_{285–298}$ and $HSP70_{113–126}$, and 21.86% and 45.07% for HTL epitopes of $HSP_{168–182}$ and $HSP70_{389–403}$, respectively in the world's population (Table 7).

Molecular Docking

The human and mouse MHC alleles used for molecular docking against the selected HSP70 peptides are shown in Table 8. Moreover, the interaction similarity scores

Table 3 The selected HTL epitopes of HSP70 protein based on binding affinity

Epitope sequence	Position	No. of alleles	Top alleles	IEDB average rank	NetMHCII average rank
NVLRIINEPTAAAIA	168–182	4	HLA-DRB1*04:01	2.2	1.75
			HLA-DRB1*04:04		
			HLA-DRB1*14:01		
			HLA-DRB1*14:02		
QDLLLLDVAPLSLGL	389–403	7	HLA-DRB1*03:01	3.01714	3.45714
			HLA-DRB1*04:01		
			HLA-DRB1*04:04		
			HLA-DRB1*04:05		
			HLA-DRB1*13:02		
			HLA-DRB1*14:01		
			HLA-DRB1*14:02		

Table 4 Antigen processing for HSP70 epitopes with two servers

Epitope	Position	NetCTL 1.2 server			IEDB server		
		C terminal cleavage affinity	TAP transport efficiency	Com (prediction score)	Proteasome score	Tap score	Processing score
FYPEEISSMVLTKM	113–126	0.918	0.457	0.3873	0.88	0.1	0.98
		0.9698	− 0.259	0.4669	0.92	0.19	1.03
		0.8997	0.143	0.3328	0.88	− 0.09	1.78
		0.1182	− 1.121	0.2161	0.92	0.28	0.83
		0.8499	0.218	0.5144	1.59		0.79
		0.9134	0.197	0.4833			
SLFEGIDFYTSITR	285–295	0.8963	3.107	0.9836	1.3	1.33	2.63
		0.1283	− 0.624	0.2191	0.78	− 0.25	0.53
		0.0987	− 2.591	0.1218	1.13	1.16	2.29
		0.8809	0.028	0.3597	1.21	0.11	1.32
		0.43	− 1.099	0.4165	1.14	− 1.1	0.04
		0.8294	1.282	0.401			

Table 5 Immunogenicity, toxicity and allergenicity of the selected HSP70 epitopes

Epitope sequence	Position	MHCI immunogenicity	Toxicity		Allergenicity
			Prediction	Score	
FYPEEISSMVLTKM	113–126	− 0.23243	Non-Toxic	− 0.72	Non-allergen
SLFEGIDFYTSITR	285–298	0.45042	Non-Toxic	− 1.43	Non-allergen
NVLRIINEPTAAAIA	168–182	–	Non-Toxic	− 1.38	Non-allergen
QDLLLLDVAPLSLGL	389–403	–	Non-Toxic	− 1.53	Non-allergen

of human and mouse MHC-I/MHC-II alleles were determined for HSP70 epitopes as shown in Tables 9, 10, 11, 12. Figures 5 and 6 are successful examples of molecular MHC-peptide docking between the selected peptides and human/mouse MHC-I and MHC-II alleles, respectively. These analyses were performed for HPV16/18 L1, L2 and E7 epitopes in our previous study [20, 33, 34].

Construct Design

The selected CTL epitopes include HPV16 L1 (^{12}YLPPVPVSKV^{21}), HPV16 L2 (^{11}KRASATQLYK^{20}), HPV16 E7 (^{216}GQAEPDRAHYNIVTF^{230}), HPV18 L1 (^{461}DQYPLGRKFLV^{471}), HPV18 L2 (^{11}KRASVTDLYK^{20}), HPV18 E7 (^{78}SSADDLRAFQQLFL^{91}), HSP70 (^{113}FYPEEISSMVLTKM^{126}), and HSP70 (^{285}SLFEGIDFYTSITR^{298}). The

Table 6 IFN-γ, IL-10 and IL-4 inducing scores of the selected HPV16/18 L1, L2, E7 and HSP70 epitopes

Protein	Epitope sequence (position)	Interferon-gamma		IL-10		IL-4	
		Result	Score	Prediction	Score	Prediction	Score
HSP70	NVLRIINEPTAAAIA (168–182)	POSITIVE	0.51194207*	IL10 inducer	0.849554409919*	Non IL4 inducer	− 0.01
HSP70	QDLLLLDVAPLSLGL (389–403)	POSITIVE	0.48938682	IL10 inducer	0.860154883862*	Non IL4 inducer	0.03
HSP70	FYPEEISSMVLTKM (113–126)	POSITIVE	0.48602662	IL10 non-inducer	.0716812685963	IL4 inducer	0.39*
HSP70	SLFEGIDFYTSITR (285–298)	POSITIVE	0.50033371	IL10 non-inducer	0.227316143198	IL4 inducer	0.40*
L1 Type16	YLPPVPVSKV (12–21)	POSITIVE	0.47010774	IL10 non-inducer	− 0.520456297282	Non IL4 inducer	0.13
L1 Type16	DTYRYVQSQAITCQK (416–430)	POSITIVE	0.45664992	IL10 inducer	0.571853145342	IL4 inducer	0.30*
L1 Type18	DQYPLGRKFLV (461–471)	POSITIVE	0.48269566	IL10 inducer	0.345065735571	IL4 inducer	0.28
L1 Type18	DNTVYLPPPSVARVV (8–22)	POSITIVE	0.51973472*	IL10 non-inducer	− 0.0234413499761	Non IL4 inducer	0.16
L2 Type16	KRASATQLYK (11–20)	POSITIVE	0.45691381	IL10 non-inducer	− 0.0202630039221	Non IL4 inducer	− 0.12
L2 Type16	PDFLDIVALHRPALTSR (281–297)	POSITIVE	0.49419964	IL10 non-inducer	− 0.0331455097738	Non IL4 inducer	0.13
L2 Type18	KRASVTDLYK (11–20)	POSITIVE	0.44888752	IL10 non-inducer	− 0.330667977025	Non IL4 inducer	0.12
L2 Type18	SDFMDIIRLHRPALTSR (274–290)	POSITIVE	0.56231739*	IL10 non-inducer	0.223762693932	IL4 inducer	0.38*
E7 Type16	GQAEPDRAHYNIVTF (216–230)	POSITIVE	0.45394927	IL10 non-inducer	0.296398886442	IL4 inducer	0.40*
E7 Type18	SSADDLRAFQQLFL (78–91)	POSITIVE	0.4714869	IL10 non-inducer	0.206064727887	Non IL4 inducer	− 0.25

*Higher rates show more potent epitopes for inducing cytokines

selected HTL epitopes contain HPV16 L1 (^{416}DTYRYVQSQAITCQK^{430}), HPV16 L2 (^{281}PDFLDIVALHRPALTSR^{297}), HPV18 L1 (^{8}DNTVYLPPPSVARVV^{22}), HPV18 L2 (^{274}SDFMDIIRLHRPALTSR^{290}), HSP70 (^{168}NVLRIINEPTAAAIA^{182}), and (^{389}QDLLLLDVAPLSLGL^{403}). These top-ranked epitopes were fused by AAY linker for design of the L1-L2-E7 and HSP70-L1-L2-E7 multiepitope peptide constructs (Fig. 3).

B-Cell Epitope Prediction

The sequences and position of the predicted B-cell epitopes are shown in Fig. 7 and Table 13. These regions had the ability to induce antibody.

Physicochemical Characteristics

Various physicochemical properties of the L1-L2-E7 and HSP70-L1-L2-E7 constructs were determined by ProtParam tool as shown in Table 14. Our results indicated that the L1-L2-E7 and HSP70-L1-L2-E7 multiepitope peptides had molecular weight (MW) of about 19.5 kDa and 28.5 kDa, respectively. Moreover, the L1-L2-E7 and HSP70-L1-L2-E7 multiepitope peptides were unstable with the instability index (II) of 41.53 and 43.63 (i.e., a value more than 40 means that the protein is not stable [64]), and also were less soluble with the probability of 0.376 and 0.301, respectively.

Secondary Structure Modeling

The secondary structure prediction of the L1-L2-E7 and HSP70-L1-L2-E7 multiepitope peptide constructs was done by PSIPRED and RaptorX servers as shown in Fig. 8. The secondary structure for the L1-L2-E7 construct was composed of 42% α-helix, 6% β-sheet, 51% coil, and 5% disordered. The secondary structure for the HSP70-L1-L2-E7 construct was composed of 43% α-helix, 17% β-sheet, 38% coil, and 3% disordered. Linkage of HSP70 epitopes changed the rates of β-sheet and coil secondary structures.

Table 7 Population coverage for the selected epitopes of HSP70 protein

Area	Population coverage HSP70-CLASSI		Population coverage HSP70-CLASSII	
	FYPEEISSMVLTKM (113–126)	SLFEGIDFYTSITR (285–298)	NVLRIINEPTAAAIA (168–182)	QDLLLLDVAPLSLGL (389–403)
Central Africa	57.42%	53.45%	4.19%	34.68%
Central America	3.37%	1.99%	25.37%	32.8%
East Africa	53.32%	55.57%	3.37%	31.94%
East Asia	85.01%	75.68%	11.61%	43.33%
Europe	87.76%	95.13%	20.75%	45.38%
Iran	78.76%	83.9%	8.69%	30.93%
North Africa	71.27%	75.45%	8.49%	43.39%
North America	82.71%	87.04%	27.12%	52.39%
Northeast Asia	79.34%	79.08%	14.09%	28.38%
Oceania	85.14%	75.38%	11.76%	24.15%
South Africa	55.96%	53.35%	1.89%	30.61%
South America	63.21%	61.26%	26.51%	38.04%
South Asia	5.96%	76.12%	13.59%	32.62%
Southeast Asia	86.93%	75.8%	14.3%	31.09%
Southwest Asia	73.34%	78.42%	8.51%	23.46%
West Africa	66.44%	66.63%	5.78%	34.47%
West Indies	84.36%	83.37%	6.99%	24.51%
World	81.19%	88.39%	21.86%	45.07%
Average	70.64%	70.33	13.7	34.85

Table 8 Human and mouse MHC alleles used for molecular docking analysis against the selected peptides

Human alleles				Mouse alleles			
MHC-I		MHC-II		MHC-I		MHC-II	
Allele	PDB	Allele	PDB	Allele	PDB	Allele	PDB
HLA-A*02:01	4UQ3	HLA-DRB1*01:01	4AH2	H-2-Ld	1LDP	H-2-IAb	4P23
HLA-A*24:02	5HGA	HLA-DRB1*03:01	2Q6W	H-2-Kd	5GSV	H-2-IAd	2IAD
HLA-A*01:01	4NQV	HLA-DRB1*04:01	5LAX	H-2-Kb	4PV9		
HLA-A*03:01	3RL2	HLA-DRB5*01:01	1FV1	H-2-Kk	1ZTV		
HLA-A*11:01	1X7Q	HLA-DRB1*11:01	5JLZ	H-2-Dd	5IVX		
HLA-B*07:02	5EO1	HLA-DRB1*15:01	5V4M	H-2-Db	1JUF		
HLA-B*08:01	3SPV						
HLA-B*27:05	1OGT						
HLA-B*35:01	3LKN						
HLA-B*51:01	1E27						
HLA-B*39:01	4O2C						
HLA-B*58:01	5IND						
HLA-A*30:01	6J1W						

3D Structure Prediction, Refinement and Validation

The assurance of each 3D model predicted by I-TASSER was calculated using C-score that is commonly in the range of − 5 to 2. A higher value of C-score shows a higher confidence for a model. The C-scores of the best model for the L1-L2-E7 and HSP70-L1-L2-E7 multiepitope peptides were − 3.66 and − 2.72, respectively. Figure 9 indicates the tertiary structures of the predicted L1-L2-E7 and HSP70-L1-L2-E7 constructs. The top model of each construct was refined by GalaxyRefine server. Then, the top refined model was validated by ERRAT server. Our results showed that the quality of 3D structure was

Table 9 Human MHC-I-peptide docking scores of the selected CTL epitopes

Epitope	model	HLA A0101		HLA A0201		HLA A0301		HLA A2402		HLA A1101		HLA B0702		HLA B0801		HLA B2705		HLA B3501		HLA B5101		HLA A3001		HLA B3901		HLA B5801	
		TM*	IS**	TM*	IS**	TM*	IS**	TM*	IS**	TM*	IS**	TM*	IS**	TM*	IS**	TM*	IS**	TM*	IS**	TM*	IS**	TM*	IS**	TM*	IS**	TM*	IS**
FYPEE-ISSMV-LTKM	1	0.917	233	0.955	255	0.919	244	0.984	255	0.915	252	0.989	236	0.994	251	0.984	228	0.995	237	1	263	0.983	236	0.985	236	0.984	230
(113–126)	2	0.989	204	0.955	255	0.919	244	0.984	255	0.992	220	0.967	239	0.98	230	0.989	221	0.982	233	1	263	0.886	246	0.906	258	0.975	219
	3	0.982	204	0.937	240	0.943	229	0.982	224	0.956	218	0.966	239	0.98	220	0.917	242	0.994	218	0.967	235	0.978	210	0.983	225	0.973	219
	4	0.989	196	0.934	241	0.933	214	0.982	224	0.975	211	0.963	237	0.929	237	0.992	202	0.966	224	0.967	235	0.944	223	0.969	227	0.992	212
	5	0.965	198	0.933	239	0.937	209	0.993	216	0.954	216	0.965	234	0.974	220	0.979	206	0.991	215	0.966	234	0.977	209	0.966	227	0.974	217
	6	0.965	198	0.956	226	0.928	212	0.993	216	0.951	216	0.909	250	0.972	220	0.975	205	0.964	224	0.966	234	0.94	221	0.967	225	0.915	236
	7	0.961	196	0.929	235	0.95	201	0.933	216	0.984	199	0.997	212	0.984	214	0.975	205	0.991	214	0.964	232	0.974	206	0.998	213	0.973	214
	8	0.966	190	0.972	216	0.941	203	0.933	216	0.985	197	0.966	212	0.959	222	0.985	201	0.964	222	0.964	232	0.946	215	0.967	222	0.985	205
	9	0.987	180	0.952	222	0.944	196	0.981	218	0.956	207	0.983	213	0.958	220	0.973	203	0.91	241	0.965	229	0.944	212	0.986	208	0.991	198
	10	0.987	179	0.862	252	0.933	197	0.992	206	0.948	204	0.975	215	0.957	220	0.973	200	0.963	219	0.965	229			0.997	201	0.984	197
SLFEGID-FYT-SITR	1	0.989	206	0.955	258	0.943	232	0.984	223	0.992	221	0.989	227	0.994	233	0.984	230	0.982	238	0.985	221	0.983	224	0.985	240	0.984	235
(285–298)	2	0.982	189	0.974	219	0.943	232	0.984	223	0.975	198	0.983	216	0.994	233	0.984	230	0.982	238	1	209	0.979	198	0.983	215	0.984	235
	3	0.989	181	0.973	215	0.919	209	0.984	223	0.915	218	0.975	206	0.974	218	0.984	230	0.995	215	0.993	200	0.978	196	0.998	192	0.984	235
	4	0.917	199	0.968	216	0.919	209	0.984	223	0.99	184	0.997	190	0.974	218	0.984	230	0.995	215	0.996	187	0.982	193	0.906	224	0.984	235
	5	0.987	172	0.972	214	0.946	190	0.981	215	0.999	181	0.978	194	0.98	215	0.989	211	0.991	215	0.996	193	0.98	193	0.97	197	0.987	192
	6	0.986	168	0.963	217	0.946	190	0.981	215	0.983	185	0.973	194	0.98	215	0.989	211	0.991	215	0.986	185	0.98	192	0.989	189	0.987	192
	7	0.982	168	0.975	208	0.942	191	0.981	215	0.984	184	0.966	196	0.98	203	0.989	211	0.994	192	0.965	192	0.972	195	0.977	193	0.987	192
	8	0.986	166	0.974	207	0.942	191	0.973	189	0.978	186	0.985	188	0.929	220	0.979	193	0.994	192	0.98	186	0.977	192	0.979	192	0.992	190
	9	0.987	165	0.969	207	0.955	185	0.973	189	0.984	182	0.965	195	0.972	203	0.979	193	0.995	191	0.947	196	0.973	193	0.989	188	0.992	190
	10	0.965	172			0.954	185	0.973	189	0.969	186	0.909	214	0.994	191	0.979	193	0.976	191	0.964	187	0.97	194	0.988	188	0.992	190

TM*: Protein structure similarity (TM-score), IS**: Interaction similarity score

Table 10 Human MHC-II-peptide docking scores of the selected HTL epitopes

Epitope	Position	model	DRB1–0101		DRB1–0301		DRB1–0401		DRB1–1101		DRB1–1501		DRB5–0101	
			TM*	IS**	TM*	IS**	TM*	IS**	TM*	IS**	TM*	IS**	TM*	IS**
NVLRIINEPTAAAIA	168–182	1	0.963	145	1	115	0.988	122	0.988	122	0.987	122	1	118
		2	0.967	133	0.977	122	0.972	116	0.97	116	0.98	116	0.985	122
		3	0.971	129	0.962	116	0.988	107	0.989	107	0.99	107	0.975	116
		4	0.988	122	0.978	107	0.983	107	0.991	100	0.993	101	0.99	107
		5	0.976	125	0.98	100	0.99	101	0.986	101	0.992	100	0.987	100
		6	0.981	116	0.977	101	0.982	104	0.989	96	0.956	111	0.982	101
		7	0.975	115	0.982	96	0.991	100	0.986	96	0.994	96	0.974	102
		8	0.991	107	0.978	96	0.989	96	0.983	97	0.989	96	0.989	96
		9	0.994	101	0.979	90	0.988	96	0.994	90	0.978	98	0.984	96
		10	0.993	100	0.965	91	0.994	90	0.983	91	0.961	103	0.956	105
QDLLLLDVAPLSLGL	389–403	1	0.963	158	1	137	0.982	127	0.994	121	0.956	134	0.992	11
		2	0.971	150	1	137	0.986	124	0.983	120	0.988	121	0.956	128
		3	0.976	148	1	137	0.994	121	0.987	116	0.987	111	0.974	118
		4	0.967	141	0.979	121	0.983	120	0.988	111	0.961	120	0.985	111
		5	0.975	133	0.979	121	0.988	111	0.988	110	0.978	110	0.99	105
		6	0.994	121	0.979	121	0.988	111	0.983	110	0.99	105	0.967	109
		7	0.961	127	0.977	111	0.988	105	0.989	105	0.978	109	0.942	118
		8	0.988	111	0.977	111	0.98	103	0.986	98	0.951	119	1	94
		9	0.969	117	0.978	105	0.981	102	0.99	96	0.951	119	0.993	96
		10	0.975	114	0.978	105	0.99	98	0.97	102	0.993	98	0.975	102

TM*: Protein structure similarity (TM-score), IS**: Interaction similarity score

Table 11 Mouse MHC-I peptide docking scores of the selected CTL epitopes

Epitope	Position	model	H-2-Ld		H-2-Kd		H-2-Kb		H-2-Kk		H-2-Dd		H-2-Db	
			TM*	IS**	TM*	IS**	TM*	IS**	TM*	IS**	TM*	IS**	TM*	IS**
FYPEEISSMVLTKM	113–126	1	1	324	0.94	318	0.975	248	0.636	− 7	0.946	259	0.991	344
		2	1	324	0.94	318	0.975	248	0.636	− 7	0.946	259	0.991	344
		3	1	324	0.94	318	0.934	254	0.636	− 11	0.968	238	0.991	344
		4	1	324	0.94	318	0.934	254	0.636	− 12	0.968	238	0.991	344
		5	1	324	0.94	318	0.939	249	0.635	− 12	0.967	234	0.991	344
		6	0.95	339	0.944	264	0.939	249	0.639	− 17	0.967	234	0.991	344
		7	0.95	339	0.944	264	0.947	243	0.637	− 21	0.962	232	0.991	344
		8	0.95	339	0.944	264	0.927	248	0.638	− 23	0.962	232	0.991	344
		9	0.95	339	0.944	264	0.936	232	0.64	− 25	0.975	227	0.991	344
		10	0.95	339	0.944	264	0.987	211	0.635	− 24	0.975	227	0.991	344
SLFEGIDFYTSITR	285–298	1	0.95	307	0.94	282	0.966	242	0.64	− 9	0.946	233	0.991	314
		2	0.95	307	0.94	282	0.966	242	0.64	− 9	0/946	233	0.991	314
		3	0.95	307	0.94	282	0.975	224	0.636	− 7	0.968	209	0.991	314
		4	1	273	0.94	282	0.975	224	0.639	− 12	0.968	209	0.991	314
		5	1	273	0.94	282	0.971	223	0.636	− 10	0.989	199	0.991	314
		6	1	273	0.94	282	0.934	229	0.636	− 12	0.989	199	0.991	314
		7	0.951	280	0.94	282	0.947	223	0.635	− 12	0.975	203	0.991	314
		8	0.951	280	0.94	282	0.987	204	0.638	− 18	0.936	212	0.991	314
		9	1	240	0.94	282	0.939	217	0.637	− 19	0.967	200	0.991	314
		10	1	240	0.94	282	0.927	219	0.635	− 32	0.962	199	0.991	314

TM*: Protein structure similarity (TM-score), IS**: Interaction similarity score

Table 12 Mouse MHC-II-peptide docking scores of the selected HTL epitopes

Epitope	Position	Model	H-2-IAb		H-2-IAd	
			TM*	IS**	TM*	IS**
NVLRIINEPTAAAIA	168–182	1	0.957	107	0.97	91
		2	0.948	107	0.98	74
		3	0.963	90	0.975	71
		4	0.955	90	0.955	79
		5	0.952	89	0.943	84
		6	0.954	83	0.943	78
		7	0.951	82	0.971	63
		8	0.943	82	0.936	78
		9	0.953	78	0.907	85
		10	0.955	77	0.938	71
QDLLLLDVAPLSLGL	389–403	1	0.953	107	0.937	108
		2	0.932	107	0.955	99
		3	0.955	99	0.943	100
		4	0.957	97	0.973	86
		5	0.916	106	0.907	107
		6	0.948	95	0.97	77
		7	0.913	104	0.938	87
		8	0.944	92	0.931	87
		9	0.963	81	0.925	88
		10	0.938	89	0.943	80

TM*: Protein structure similarity (TM-score), IS**: Interaction similarity score

improved after refinement process as shown in Table 15 and Fig. 10.

Molecular Docking Between the Multiepitope Peptides and TLRs

Molecular docking between the multiepitope constructs and TLRs was done using ClusPro 2.0. After prediction, we selected the models which properly occupied the receptor and had the lowest energy scores. The lowest energy level obtained for TLR-2-L1-L2-E7, TLR-3-L1-L2-E7, TLR-4-L1-L2-E7, TLR-5-L1-L2-E7, TLR-8-L1-L2-E7 and TLR-9-L1-L2-E7 constructs was −839.0, −957.8, −908.0, −1210.0, −929.0, and −1034.0, respectively as shown in Fig. 11. The lowest energy level achieved for TLR-2-HSP70-L1-L2-E7, TLR-3-HSP70-L1-L2-E7, TLR-4-HSP70-L1-L2-E7, TLR-5-HSP70-L1-L2-E7, TLR-8-HSP70-L1-L2-E7 and TLR-9-HSP70-L1-L2-E7 constructs was −929.0, −1064.0, −974.3, −1249.1, −990.2, −1034.0, respectively as shown in Fig. 12. The lowest energy levels determine the highest binding affinity between all of the predicted docked complexes.

In Vitro Experiments

Confirmation of the Plasmid DNA

At first, the pUC-57 vector harboring the HSP70-L1-L2-E7 fusion DNA construct (Fig. 13) was designed and synthesized. Then, the L1-L2-E7 and HSP70-L1-L2-E7 genes were successfully subcloned into pEGFP-N1 and pcDNA3.1 (-) eukaryotic vectors. After digestion, the L1-L2-E7 and HSP70-L1-L2-E7 genes with the clear bands of ~ 519 bp and ~ 753 bp were confirmed on agarose gel, respectively (Fig. 14).

Expression of the L1-L2-E7 and HSP70-L1-L2-E7 Genes In Vitro

The DNA constructs (pEGFP-L1-L2-E7 and pEGFP-HSP70-L1-L2-E7) were transfected into the eukaryotic cell line (HEK-293T) using TurboFect transfection reagent. The data showed that the cellular uptake of pEGFP-L1-L2-E7 and pEGFP-HSP70-L1-L2-E7 into the

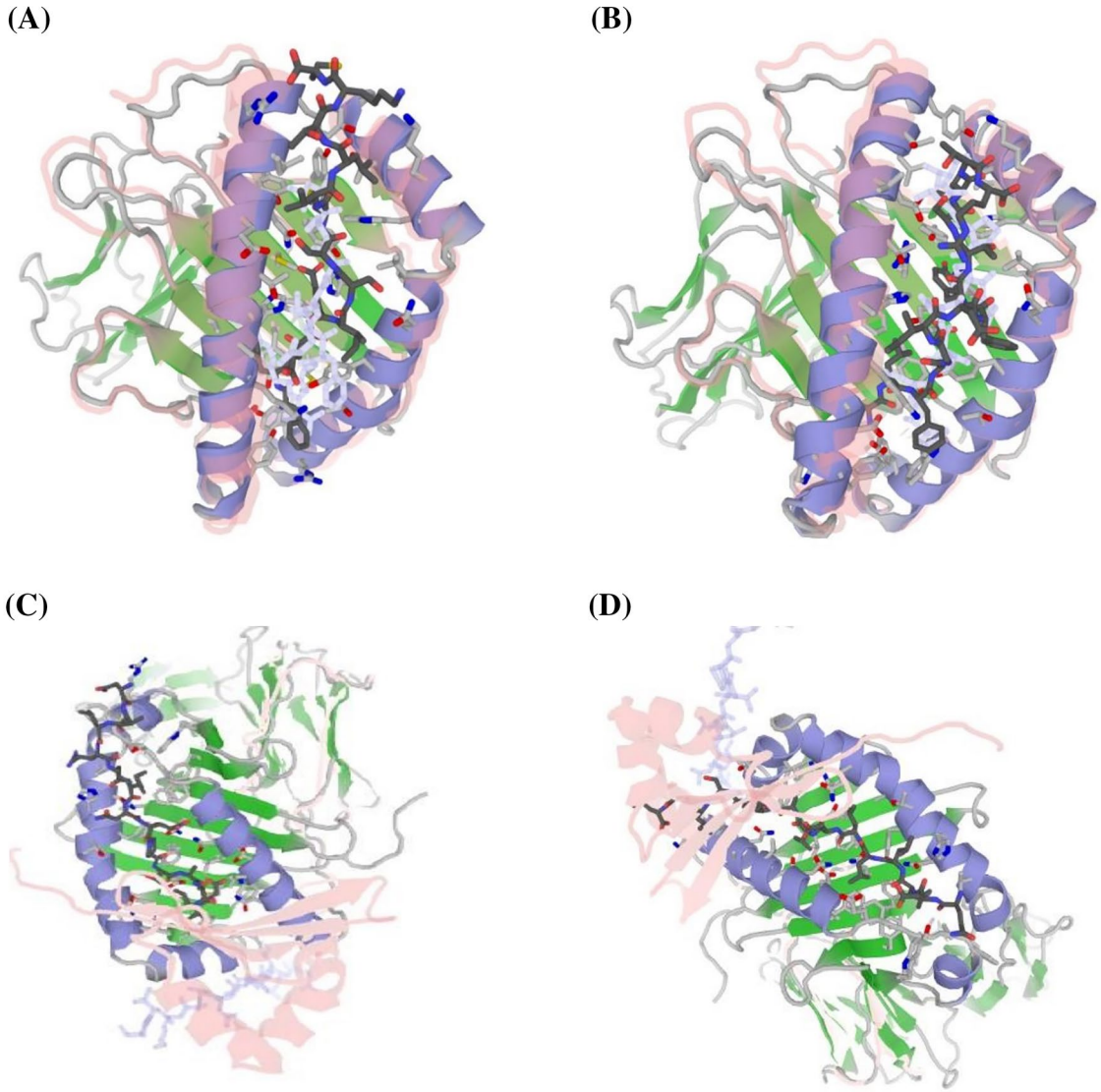

Fig. 5 Peptide-MHC docking between the selected epitopes of HSP70 and human MHC alleles: **A** The successful docking between ^{113}FYPEEISSMVLTKM^{126} and HLA-A2402 with interaction score of 255.0; **B** The successful docking between ^{285}SLFEGIDFYTSITR^{298} and HLA-A0201 with interaction score of 258.0; **C** The successful docking between ^{168}NVLRIINEPTAAAIA^{182} and DRB1-0101 with interaction score of 145.0; **D** The successful docking between ^{389}QDLLLLDVAPLSLGL^{403} and DRB1-0101with interaction score of 158.0

HEK-293T cells was ~ 56.16% ± 0.31 and ~ 80.45% ± 0.81, respectively. Moreover, the green cells were detected for the L1-L2-E7 and HSP70-L1-L2-E7 DNA delivery in HEK-293T cells using fluorescent microscopy (Fig. 15). The successful expression of the L1-L2-E7 and HSP70-L1-L2-E7 multiepitope peptides fused to GFP was confirmed by Western blotting, as well. Our results showed the clear bands of ~ 46.5, ~ 55.5 and ~ 27 kDa for the L1-L2-E7-GFP, HSP70-L1-L2-E7-GFP and GFP constructs, respectively (Fig. 16).

In Vivo Studies

Preventive Study

Antibody Assay The levels of total IgG, IgG1 and IgG2a in mice immunized with the HSP70-L1-L2-E7 DNA construct (G2) was significantly higher than other groups against both L1-L2-E7 and HSP70-L1-L2-E7 multiepitope peptides as antigens ($p < 0.05$, Fig. 17). In addition, the levels of IgG2a in groups immunized with the HSP70-L1-L2-E7 (G2) and

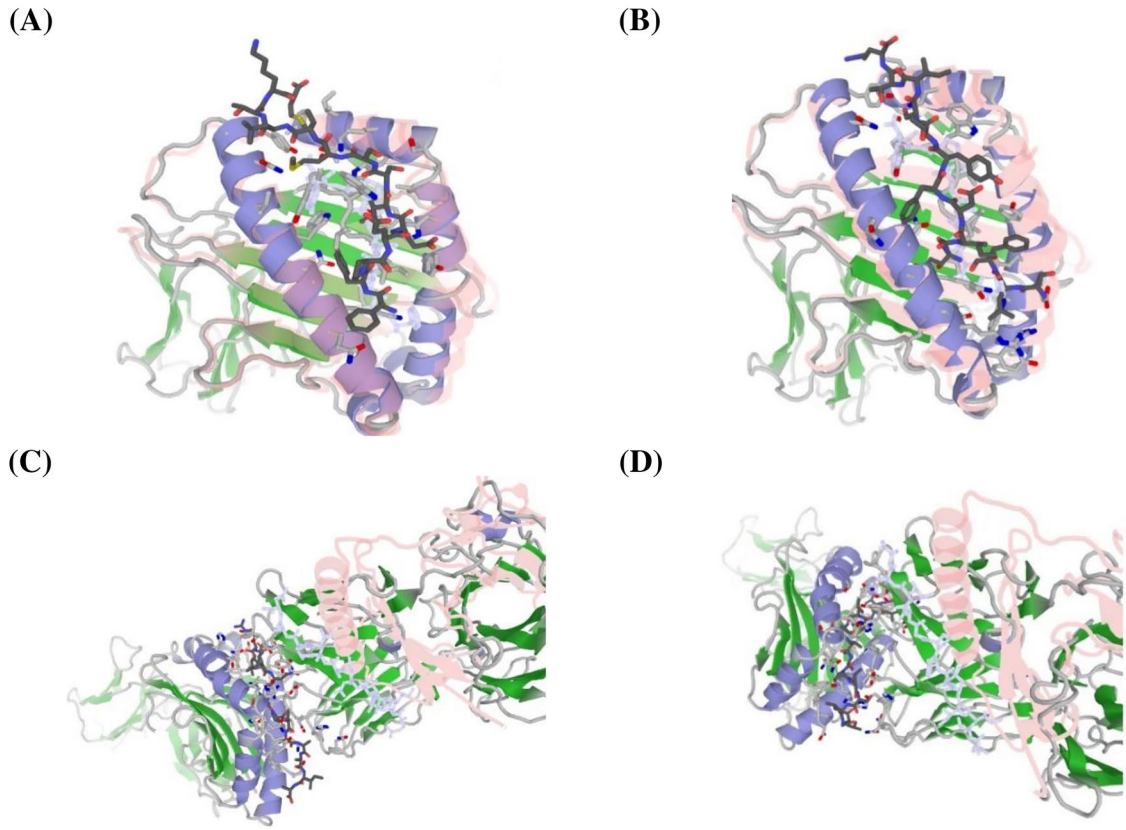

Fig. 6 Peptide-MHC docking between the selected epitopes of HSP70 and mouse MHC alleles: **A** The successful docking between ^{113}FYPEEISSMVLTKM^{126} and H-2-Db with interaction score of 344.0; **B** The successful docking between ^{285}SLFEGIDFYTSITR^{298} and H-2-Db with interaction score of 314.0; **C** The successful docking between ^{168}NVLRIINEPTAAAIA^{182} and H-2-IAb with interaction score of 107.0; **D** The successful docking between ^{389}QDLLLLDVAPLSLGL^{403} and H-2-IAb with interaction score of 107.0

L1-L2-E7 (G1) DNA constructs were significantly higher than the levels of IgG1 especially against the HSP70-L1-L2-E7 multiepitope peptide as an antigen ($p < 0.05$). No significant antigen-specific antibody response was observed in the control sera.

Cytokine Detection As detected, the levels of IFN-γ and IL-4 secretion in groups immunized with the L1-L2-E7 (G1) and HSP70-L1-L2-E7 (G2) DNA constructs were drastically higher than control groups ($p < 0.05$, Fig. 18). In addition, the injection of the HSP70-L1-L2-E7 (G2) DNA construct increased significantly IFN-gamma response compared to the injection of L1-L2-E7 (G1) DNA construct ($p < 0.05$). In contrast, there was no significant difference in IL-4 secretion between groups immunized with the HSP70-L1-L2-E7 and L1-L2-E7 DNA constructs (G1 & G2; $p > 0.05$). Furthermore, our results indicated that the ratios of IFN-γ/IL-4 were higher in test groups (G1 & G2) than control groups; therefore, they could induce Th1 immune response. On the other hand, no significant difference was observed in IL-10 secretion between different groups (test groups compared to control groups; $p > 0.05$, data not shown).

Granzyme B Secretion The secretion of Granzyme B in groups immunized with the HSP70-L1-L2-E7 and L1-L2-E7 DNA constructs (G1 and G2) was considerably higher than the control groups ($p < 0.001$, Fig. 19). The group immunized with the HSP70-L1-L2-E7 DNA construct (G2) produced significantly higher levels of Granzyme B than other group (G1, $p < 0.001$) against both antigens.

Evaluation of Tumor Growth To determine the preventive effects of the designed L1-L2-E7 and HSP70-L1-L2-E7 DNA constructs, tumor growth and survival rate were determined for 65 days after C3 challenge. The groups immunized with the L1-L2-E7 and HSP70-L1-L2-E7 DNA constructs (G1 & G2) indicated drastically lower tumor growth than that in control groups (G3 & G4, $p < 0.01$; Fig. 20A). Tumor growth was observed in control groups on approximately 7–14 days. The group vaccinated with the HSP70-L1-L2-E7 DNA construct (G2) reduced tumor growth more than the group immunized with the L1-L2-E7 DNA construct (G1) but it was not significant ($p > 0.05$; Fig. 20A). In addition, the group immunized with the HSP70-L1-L2-E7 DNA construct

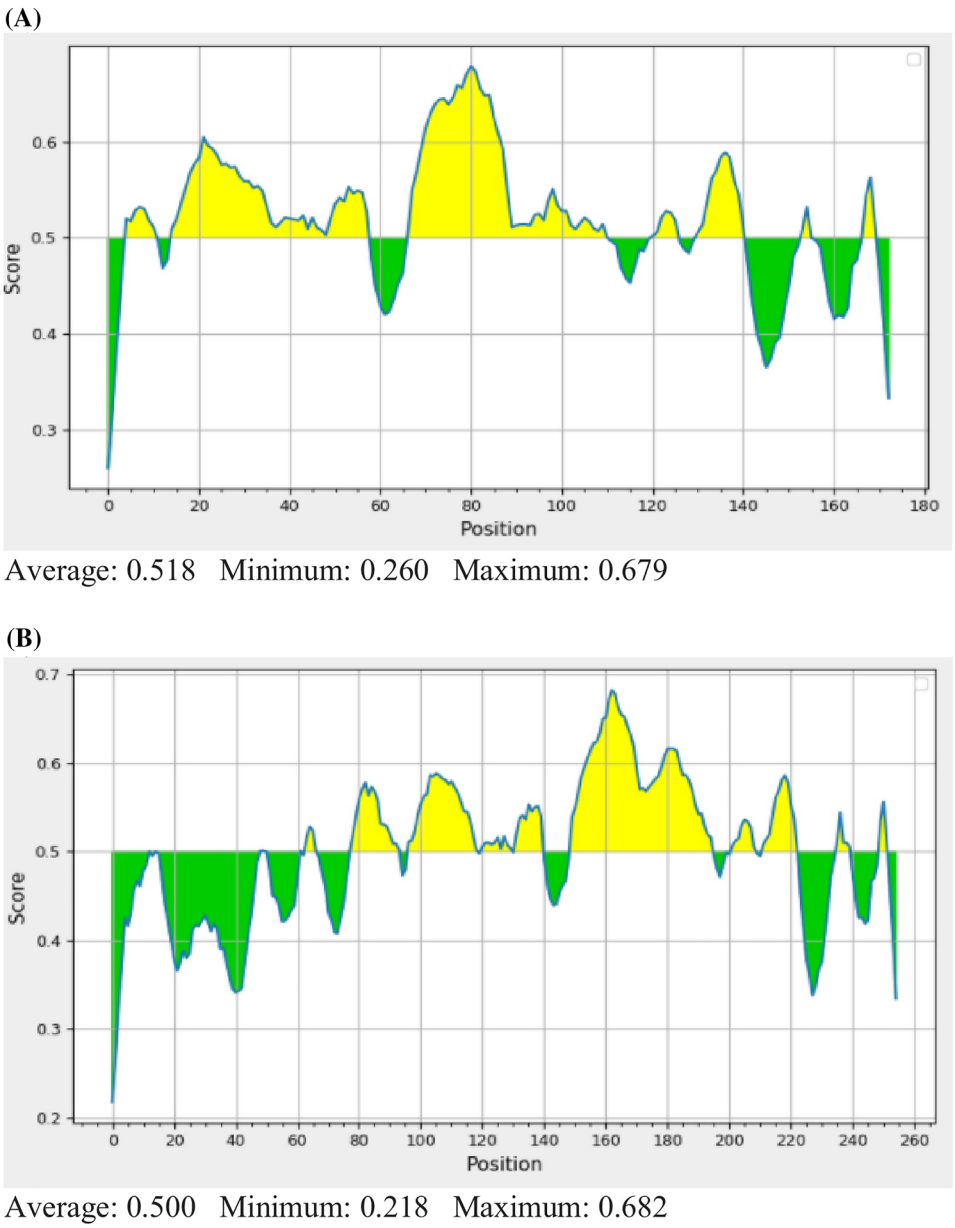

Fig. 7 Linear B-cell epitopes predicted in the designed constructs: **A** the L1-L2-E7 multiepitope construct; **B** the HSP70-L1-L2-E7 multiepitope construct. The residues with higher scores than the threshold were predicted as a part of an B-cell epitope (yellow color)

(G2) indicated a higher survival percentage (~ 80%) than the group immunized with the L1-L2-E7 DNA construct (G1; ~ 60%; Fig. 20B).

Therapeutic Effects Mice with the established tumors (~ 2–3 mm^3) were treated by the L1-L2-E7 and HSP70-L1-L2-E7 DNA constructs. Among these groups, the group vaccinated by the HSP70-L1-L2-E7 DNA construct showed a higher survival rate (G2, ~ 80%) than the L1-L2-E7 DNA construct (G1, ~ 60%) and control groups (G3 & G4, 0%) 65 days following treatment. This result was similar to the preventive effects. Indeed, the tumor growth was stopped in 80% and 60% of the treated mice (G2 & G1, respectively). As shown in Fig. 20C, groups immunized with the DNA constructs (G1 & G2) indicated significantly lower tumor growth than that in control groups (G3 & G4, $p < 0.01$).

Discussion

The HPV L1/L2 capsid proteins and E7 oncoprotein are suitable targets for the prevention and treatment of cervical cancer, respectively. The design of DNA- or peptide-based vaccine constructs containing both T- and B-cell epitopes results in boosting the strength and durability of immune responses [11, 15, 65, 66]. HSPs have been utilized as a potent adjuvant in immunotherapy of cancers and infectious diseases. Moreover, constructing an antigen-HSP fusion

Table 13 The selected linear and conformational epitopes for L1-L2-E7 (A) and HSP70-L1-L2-E7 (B) constructs

NO	Start	End	Peptide	Length
(A) Predicted peptides for L1-L2-E7				
1	5	11	DTYRYVQ	7
2	15	58	ITCQKAAYYLPPVPVSKVAAYDNTVYLPPPSVARVVAAYDQYPL	44
3	67	110	YPDFLDIVALHRPALTSRAAYSDFMDIIRLHRPALTSRAAYKRA	44
4	121	126	KRASVT	6
5	131	141	AAYGQAEPDRA	11
6	154	156	ADD	3
7	168	170	HHH	3
(B) Predicted peptides for HSP70-L1-L2-E7				
1	49	51	GID	3
2	62	62	F	1
3	64	67	PEEI	4
4	78	94	YEFRSMAAYDTYRYVQS	17
5	97	119	ITCQKAAYYLPPVPVSKVAAYDN	23
6	121	130	VYLPPPSVAR	10
7	132	140	VAAYDQYPL	9
8	150	195	PDFLDIVALHRPALTSRAAYSDFMDIIRLHRPALTSRAAYKRASAT	46
9	202	209	YKRASVTD	8
10	212	223	KAAYGQAEPDRA	12
11	236	240	ADDLR	5
12	250	252	HHH	3

Table 14 Physicochemical characteristics of two designed constructs

	HSP70-L1-L2-E7	L1-L2-E7
Theoretical pI	8.73	9.50
Molecular weight (MW.)	28536.65	19575.33
Instability index (II)	43.63(unstable)*	41.53(unstable)*
GRAVY	0.026	− 0.207
Solubility	0.301 (less soluble)**	0.376 (less soluble) **
No. of amino acids	255	173
Total no. of positively charged residues (Arg + Lys)	24	20
Total no. of negatively charged residues (Asp + Glu)	21	12
Aliphatic index	92.08	83.70
Half-life in *E. coli*, in vivo	> 10 h	> 10 h
Half-life in mammalian reticulocytes, in vitro	30 h	30 h
Half-life in yeast, in vivo	> 20 h	> 20 h

*A protein whose instability index is smaller than 40 is predicted as stable, a value above 40 predicts that the protein may be unstable

**The scaled solubility value greater than 0.45 is predicted to be high soluble and lower than 0.45 is predicted to be less soluble

provides a promising approach to enhance the potency of DNA-, protein- or peptide-based vaccines [29, 36, 67]. On the other hand, to overcome the low immunogenicity of the peptide-based vaccines, immunobioinformatics tools are beneficial in determining novel and potent antigenic epitopes [68, 69]. The immunogenicity of L1, L2 and E7 epitopes in peptide-based vaccines was evaluated in a wide-range of studies. Feltkamp et al. determined the HPV16 E7 ^{49}RAHYNIVTF^{57} sequence as an MHC-I binding epitope which triggers CTL-mediated responses [63, 70]. About 10 years later, Kawana et al. introduced HPV16 L2 peptide (^{108}VEETSFIDAGAP^{120}) as a highly immunogenic epitope [71]. Hitzeroth and Kwak showed that L2 DNA vaccination inhibited the growth of L2-expressing C3 tumor

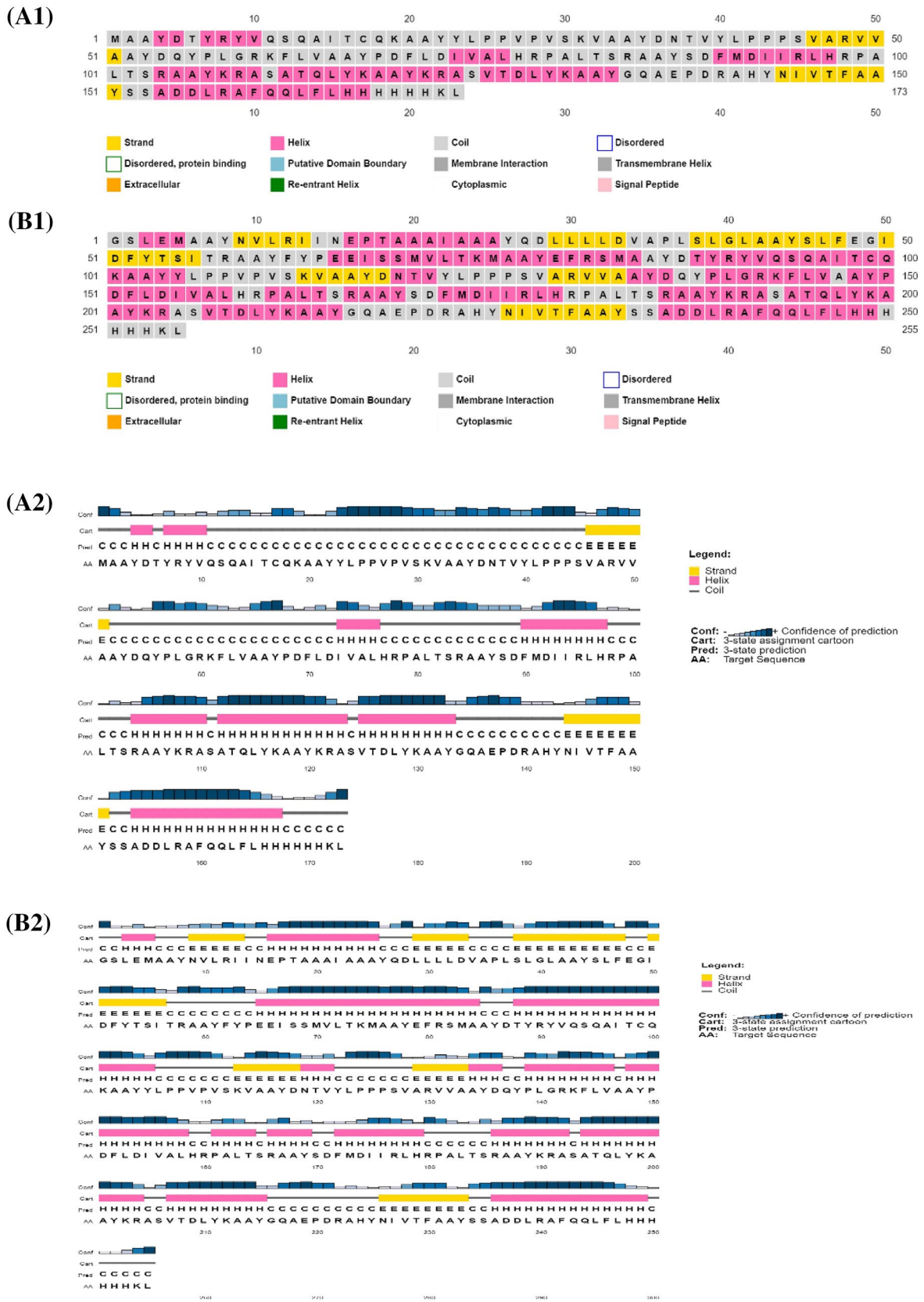

Fig. 8 The secondary structure of the designed L1-L2-E7 (**A1**, **A2**) and HSP70-L1-L2-E7 (**B1**, **B2**) constructs by PSIPRED server

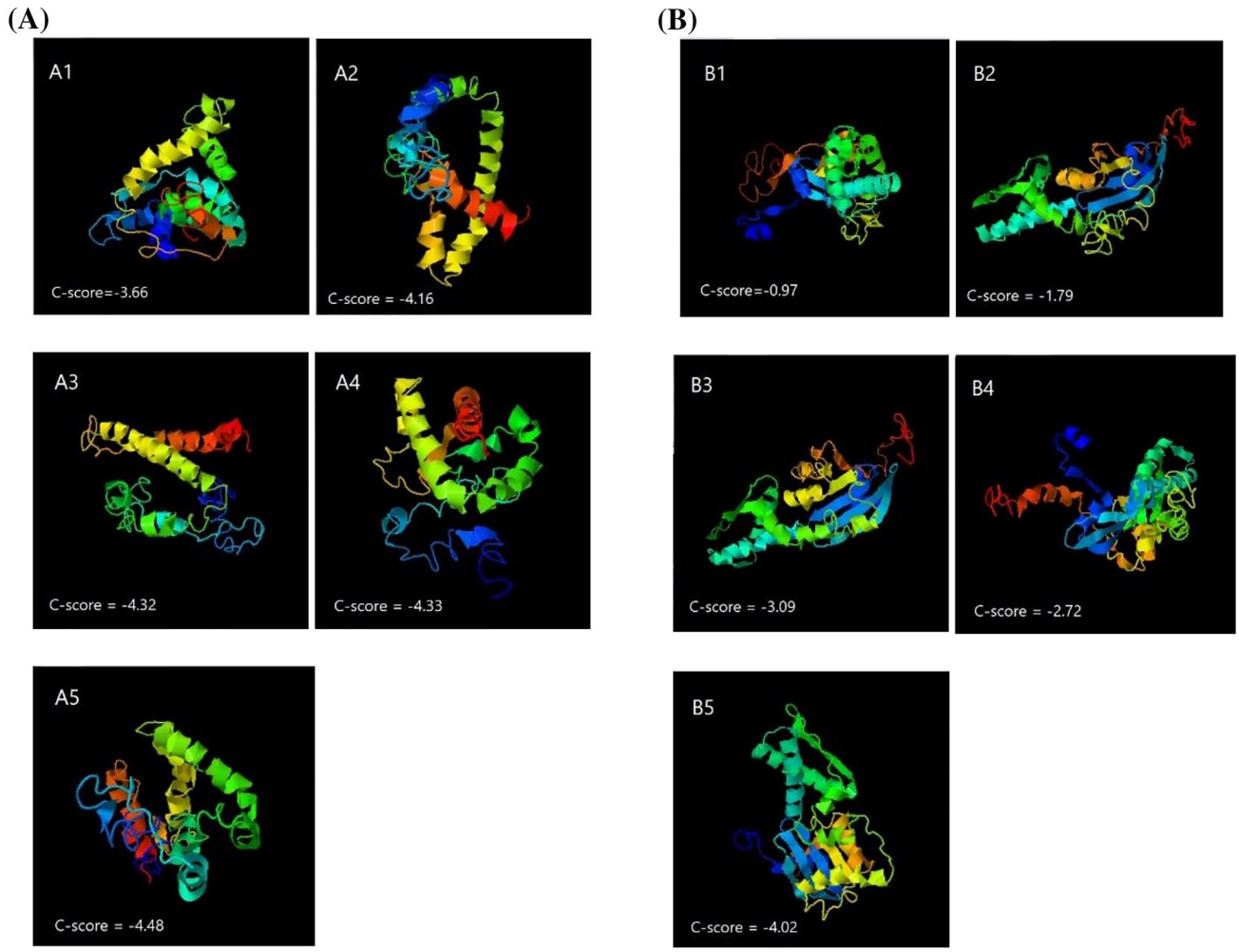

Fig. 9 The 3D structures of the L1-L2-E7 (**A**) and HSP70-L1-L2-E7 (**B**) constructs predicted by I-TASSAR server: **A** The L1-L2-E7 construct with C-score of -3.66 has the highest score among the predicted structures; **B** The HSP70-L1-L2-E7 construct with C-score of − 2.72 has the highest score among the predicted structures

Table 15 Validation of the tertiary structures

Construct	Model	Overall quality factor
L1-L2-E7	Model1	77.5758
	Model2	80.6061
	Model3	64.2424
	Model4	76.9697
	Model5	70.9091
HSP70-L1-L2-E7	Model1	69.9187
	Model2	81.3008
	Model3	76.4228
	Model4	84.1463
	Model5	70.6122

cells [72]. On the other hand, multivalent L1 DNA vaccines could induce strong cellular and humoral immune responses [73, 74]. Moreover, chimeric L1 vaccines harboring cross-neutralizing L2 peptides (e.g., ^{17}QLYKTCKQAGTCPPDI-IPKV^{36} epitope) were suggested as promising second-generation prophylactic HPV vaccine candidates [75]. In 2015, an immunogenic HPV16 L2 epitope (^{12}RASATQLYKTCK-QAGTCPPDIIPKVEGKTI^{41}) was introduced into the adenovirus 5 (Ad5) hexon as a practical method of generating a protective HPV vaccine [76]. In 2018, two 9-mer epitopes of HPV58 E7 including QAQPATANY and SSDEDEIGL were found as the most potential B- and T-cell epitopes, respectively [77]. Tsang et al. proposed six immunogenic epitopes of HPV16 E6 and E7 proteins including ^{11}KLPQLCTEL^{19}, ^{72}KISEYRHYC^{80}, ^{90}QQYNKPLCDL^{99} from E6 protein, and ^{11}YMLDLQPET^{19}, ^{7}TLHEYMLDL^{15}, ^{77}RTLEDLLMGT^{86} from E7 protein [78].

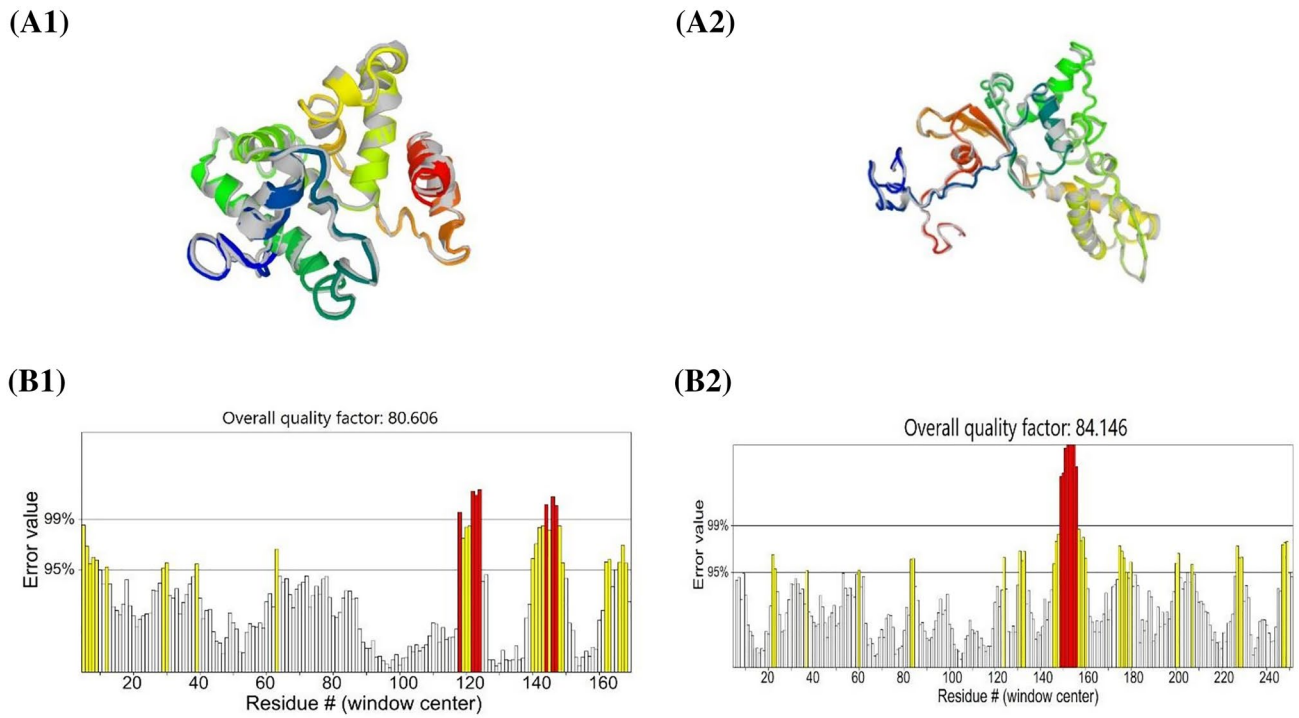

Fig. 10 The refined L1-L2-E7 (**A1**) and HSP70-L1-L2-E7 models (**A2**) generated by GalaxyRefine Server; **B1** ERRAT error values chart and quality factor of L1-L2-E7 was 80.60; **B2** ERRAT error values chart and quality factor of HSP70-L1-L2-E7 was 84.14

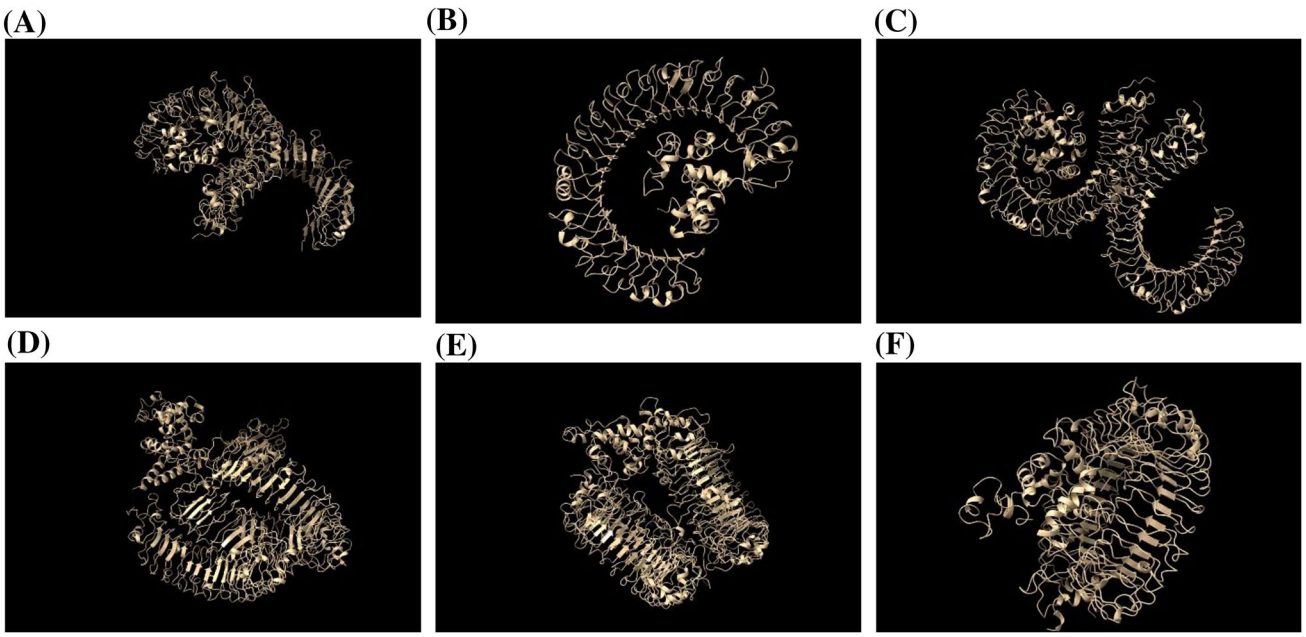

Fig. 11 The molecular docking between the L1-L2-E7 multiepitope construct and TLR-2 (**A**), TLR-3 (**B**), TLR-4 (**C**), TLR-5 (**D**), TLR-8 (**E**) & TLR-9 (**F**)

Our group previously determined the immunogenic and conserved epitopes of L1 and L2 proteins among the high-risk HPV types with the population coverage rates of 95.55% and 96.33%, respectively in worldwide [20]. In addition, we determined the immunogenic epitopes of E5, E6 and E7 oncoproteins from HPV-16, -18, -31 and -45

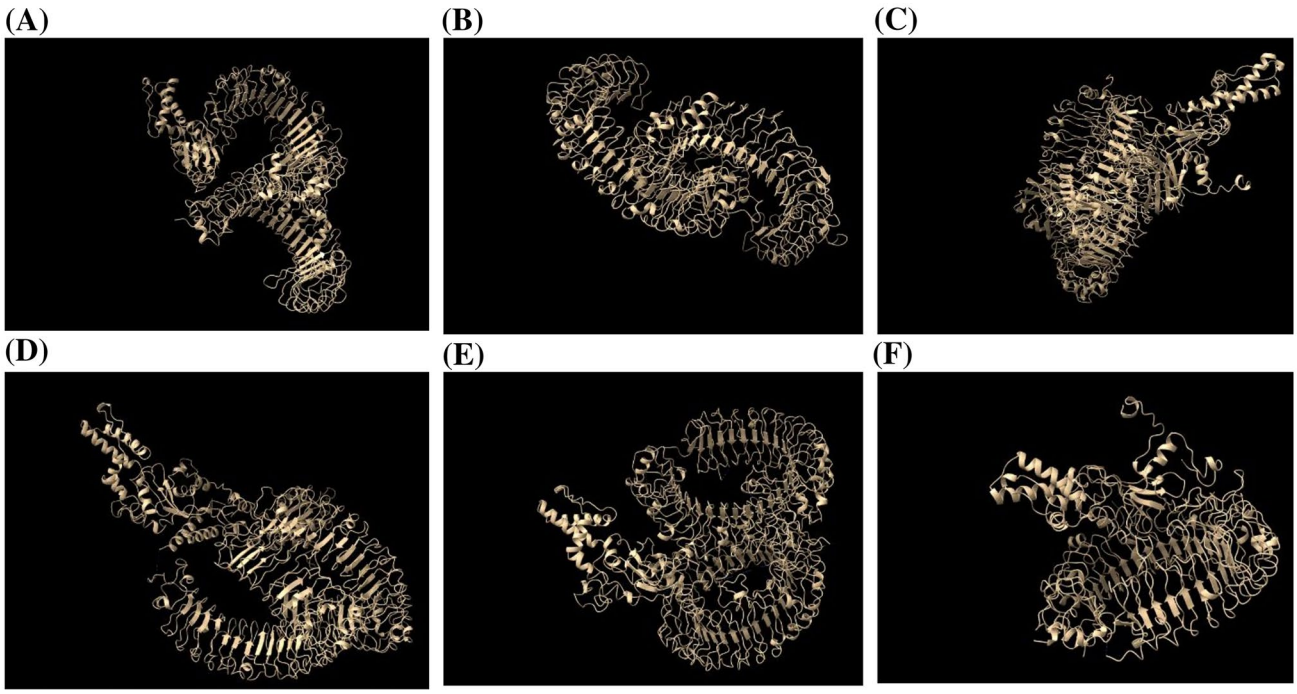

Fig. 12 The molecular docking between the HSP70-L1-L2-E7 multiepitope construct and TLR-2 (**A**), TLR-3 (**B**), TLR-4 (**C**), TLR-5 (**D**), TLR-8 (**E**) & TLR-9 (**F**)

using a two-stage immunoinformatics method [33, 34]. In this study, we used the same epitopes of L1, L2 and E7 obtained from our previous studies [20, 33, 34], and designed a L1-L2-E7 multiepitope peptide construct for further in silico studies (e.g., B-cell epitope prediction, physicochemical characteristics, secondary structure modeling, 3D structure prediction, 3D structure refinement and validation, and binding prediction to TLRs). On the other hand, different computational tools were utilized to design an additional novel multiepitope peptide construct based on the immunodominant T-cell epitopes of HSP70 linked to the L1-L2-E7 multiepitope peptide construct.

Some studies showed that the efficiency of DNA vaccines can be enhanced by the linkage of HPV16 E7 gene to HSP70 gene. For example, the fusion of *Mycobacterium tuberculosis* HSP70 (MtHSP70) to the modified HPV 16 E7 (mE7) gene stimulated a stronger E7-specific $CD8^+$ T-cell response, and a more significant therapeutic effect against E7-expressing tumor cells than the E7 DNA construct in mice [79, 80]. Also, Jiang et al. generated a recombinant protein vaccine based on the fusion of HSP70 to a melanoma tumor antigen (Mage-a1). The Mage-a1-HSP70 fusion construct could significantly increase immune responses and antitumor effects against Mage-a1-expressing tumors as compared to the Mage-a1 protein, and the combination of Mage-a1 + HSP70 proteins [29]. In 2019, Matsui et al. identified twenty-nine HSP70-derived peptides (9-mers) bound to HLA-class I using peptide-binding experiments [81].

In our study, the prediction of MHC-I and MHC-II binding HSP70 epitopes was analyzed using IEDB, NetMHCpan 4.1, and NetMHCIIpan. Hence, T-cell epitopes with the highest binding affinity scores were selected. Generally, the MHC-II binding epitopes included HPV16 L1 (^{416}DTYRYVQSQAITCQK^{430}), HPV18 L1 (^{8}DNTVYLPPPSVARVV^{22}), HPV16 L2 (^{281} PDFLDIVALHRPALTSR^{297}), HPV18 L2 (^{274}SDFMDIIRLHRPALTSR^{290}), HSP70 (^{168}NVLRIINEPTAAAIA^{182}), and HSP-70 (^{389}QDLLLLDVAPLSLGL^{403}). The MHC-I binding epitopes included HPV16 L1 (^{12}YLPPVPVSKV^{21}), HPV18 L1 (^{461}DQYPLGRKFLV^{471}), HPV16 L2 (^{11}KRASATQLYK^{20}), HPV18 L2 (^{11}KRASVTDLYK^{20}), HPV16 E7 (^{43}GQAEPDRAHYNIVTF^{57}), HPV18 E7 (^{78}SSADDLRAFQQLFL^{91}), HSP70 (^{113}FYPEEISSMVLTKM^{126}), and HSP70 (^{285}SLFEGIDFYTSITR^{298}).

The predicted HSP70 epitopes showed a high quality of proteasomal cleavage and Tap transport efficiency, as well. These epitopes were non-allergen using AlgPred server. In the next step, the population coverage rates for CTL and HTL epitopes were studied in sixteen-specified geographical regions for the predicted HSP70 epitopes. These data suggested a specific binding of the CTL and HTL epitopes to the prevalent HLA molecules in the targeted populations. For example, the highest world's population coverage for

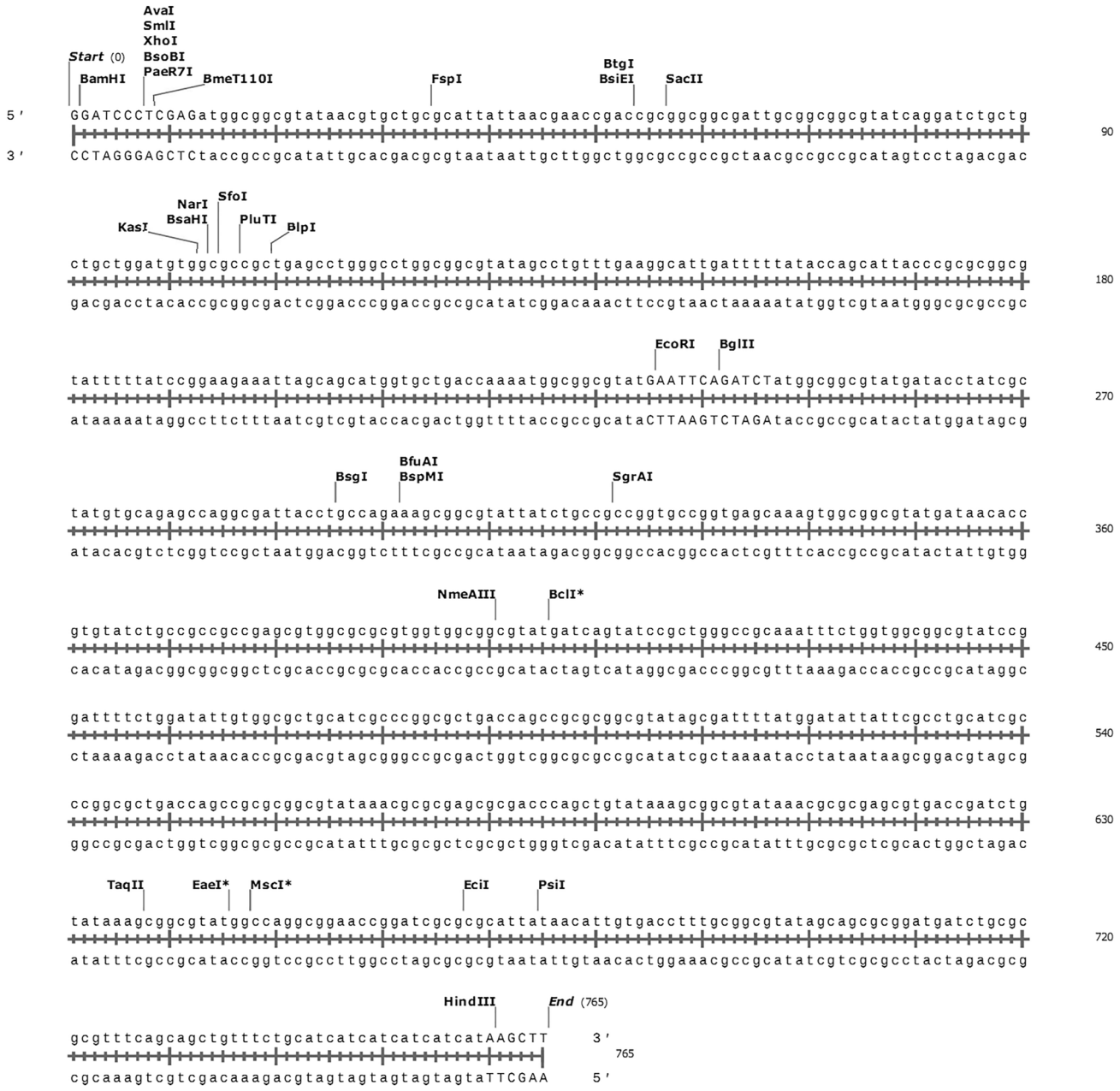

Fig. 13 The multiepitope HSP70-L1-L2-E7 DNA construct with the restriction enzymes sites

two CTL epitopes of HSP70 was calculated about 88.39% and 81.19%, and for two HTL epitopes of HSP70 were determined about 40.07% and 21.86%. Furthermore, the MHC-I binding HSP70 epitopes (113–126 and 285–298 epitopes), and the MHC-II binding HSP70 epitopes (168–182 and 389–403 epitopes) showed the highest docking scores as compared to other HSP70 epitopes. In addition, all selected epitopes of L1, L2, E7 and HSP70 could induce IFN-gamma cytokine. As known, IFN-gamma has a major role in intracellular immunity against HPV infection [82]. Finally, the L1-L2-E7 and HSP70-L1-L2-E7 multiepitope peptide constructs were designed. In the next step, further immunoinformatics tools were applied to determine some physicochemical, structural and immunological properties of the designed constructs. The physicochemical properties of the L1-L2-E7 and HSP70-L1-L2-E7 constructs indicated that they were unstable and less soluble. In addition, the L1-L2-E7 construct with molecular weight 19.5 kDa and 173 amino acids had 20 positive charge residues (Arg + Lys) and 12 negative charge residues (Asp + Glu) and the HSP70-L1-L2-E7 construct with molecular weight 28.5 kDa and 255 amino acids consisted of 24 positive and 21 negative charge

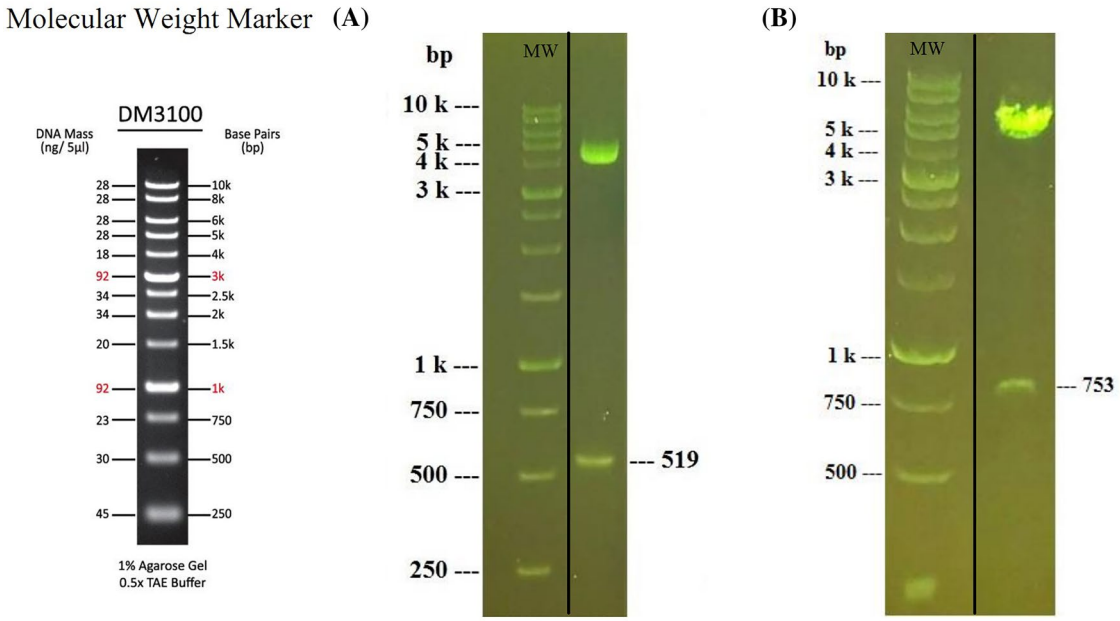

Fig. 14 Confirmation of the DNA constructs on agarose gel: **A** the pEGFP-L1-L2-E7 digested by the restriction enzymes shows a clear band of ~ 519 bp related to the L1-L2-E7 gene; **B** the pEGFP-HSP70-L1-L2-E7 digested by the restriction enzymes shows a clear band of ~ 753 bp related to the HSP70-L1-L2-E7 gene

residues. The 3D modeling of the L1-L2-E7 and HSP70-L1-L2-E7 constructs using I-TASSER server showed that the C-scores of the best models for the L1-L2-E7 and HSP70-L1-L2-E7 constructs were − 3.66 and − 2.72, respectively. These data determined that the accuracy of the HSP70-L1-L2-E7 construct was higher than the L1-L2-E7 construct. The overall quality scores of the improved models for the L1-L2-E7 and HSP70-L1-L2-E7 constructs were 80.60, and 84.14, respectively after refinement. On the other hand, the molecular docking between the multiepitope peptide constructs and TLRs showed strong interactions between them using ClusPro server. In this line, several studies showed that simultaneous activation of multiple pathways of TLRs induced by vaccines led to stronger immunogenicity effects. Activation of TLRs signaling pathways could induce inflammatory reactions as well as promote DC maturation, HTL differentiation and production of an acquired immune response [83, 84]. The activation of TLRs by various ligands plays a major role in the development of cervical cancer. It was found that E7 oncoprotein can activate the PI3K/Akt/mTOR signaling pathway through TLRs in HPV-infected host epithelial cells. The expression levels of TLR2 and TLR4 were higher in cervical cancer cells than normal cells. In addition, TLR4, TLR5 and TLR9 were strongly related to HPV infection and cervical cancer. Thus, the TLR agonists were used for vaccine design in some studies [85–87].

Following the design of HSP70-L1-L2-E7 multiepitope peptide construct, it was reversely translated to the HSP70-L1-L2-E7 multiepitope DNA construct. After synthesis of the HSP70-L1-L2-E7 multiepitope gene in the cloning vector (pUC57), the L1-L2-E7 (~ 519 bp) and HSP70-L1-L2-E7 (~ 753 bp) genes were subcloned from pUC57-HSP70-L1-L2-E7 into pEGFP-N1 and pcDNA3.1 (-) eukaryotic expression vectors for in vitro and in vivo studies, respectively. For in vitro gene expression, the recombinant pEGFP-L1-L2-E7 and pEGFP-HSP70-L1-L2-E7 were transfected into HEK-293T cells using TurboFect reagent. The flow cytometry analysis showed that the L1-L2-E7 and HSP70-L1-L2-E7 genes were expressed about ~ 56.16% ± 0.31 and ~ 80.45% ± 0.81, respectively into the cells. Also, the expression of the L1-L2-E7 and HSP70-L1-L2-E7 multiepitope peptides fused to GFP was detected as the clear bands of ~ 46.5 and ~ 55.5 kDa, respectively by Western blotting.

The reports indicated that therapeutic HPV DNA vaccines possess effective antitumor activity. GX-188E is a HPV16/18 E6/E7 DNA therapeutic vaccine (Genexine, Inc.) achieved to phase II clinical trial. Moreover, VGX-3100 is a DNA vaccine containing two plasmids encoding the consensus HPV16/18 E6 and E7 genes achieved to phase III clinical trial [66, 88]. On the other hand, several strategies were used to increase the efficiency of DNA vaccines such as the use of various adjuvants (e.g., HSPs). Some studies focused on developing the effective DNA vaccines using different regions of HSPs (e.g., the N- or C-terminal fragments) in animal models [36]. Moreover, the multi-antigenic DNA constructs were used to boost immune responses, and generate both preventive and therapeutic effects. For example, a therapeutic HPV16 E7 DNA vaccine construct encoding

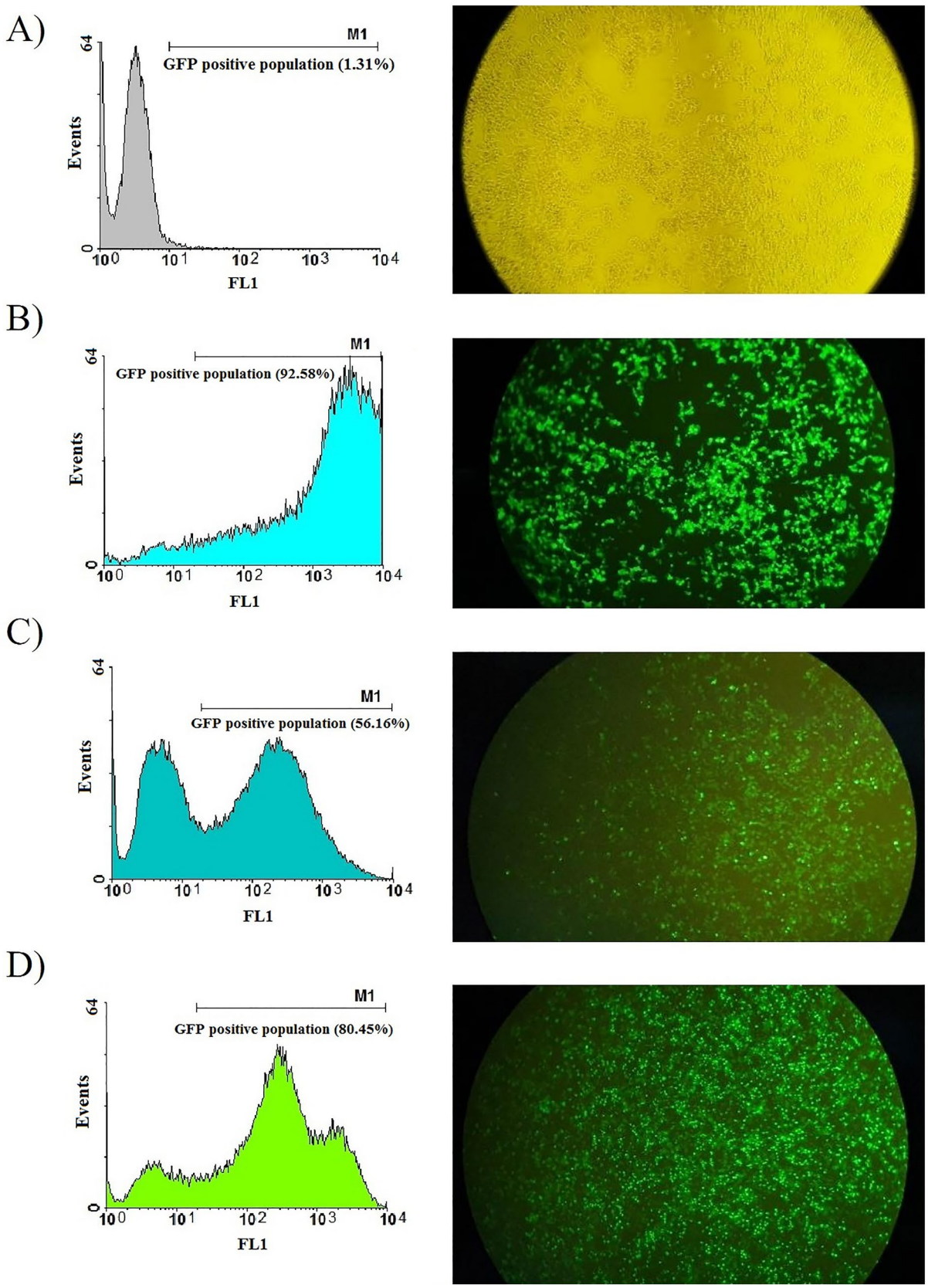

Fig. 15 Evaluation of the GFP (**B**), L1-L2-E7-GFP (**C**) and HSP70-L1-L2-E7-GFP (**D**) DNA delivery into HEK-293T mammalian cells using TurboFect. Transfection efficiency was monitored by flow cytometry (right) and fluorescent microscopy (left) at 48 h post-transfection as compared to the untransfected cells as a negative control (**A**)

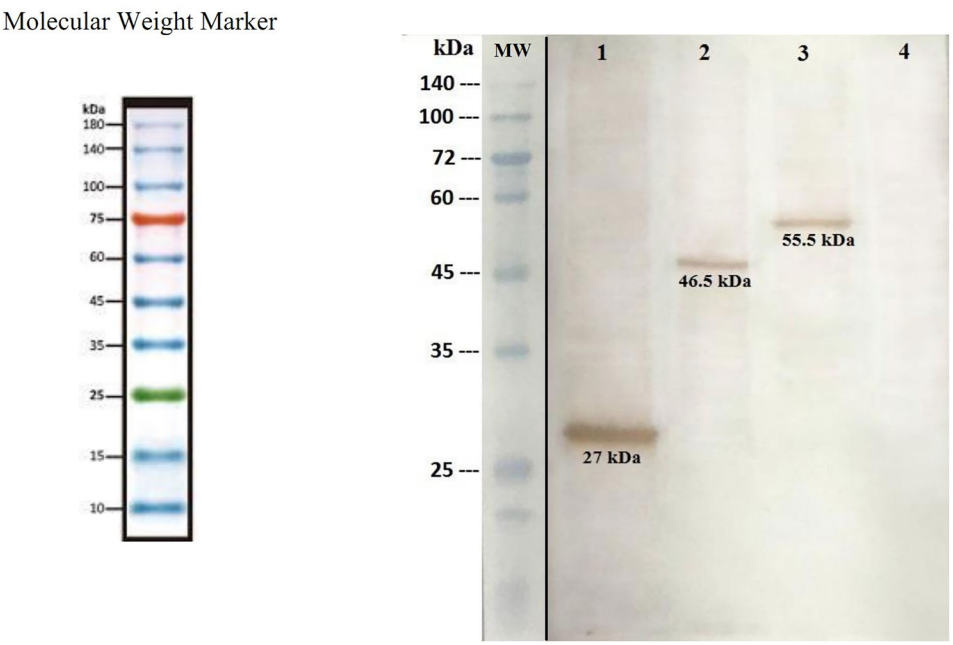

Fig. 16 Identification of protein expression in HEK-293T cells using Western blotting: The clear bands were observed for GFP (lane 1, ~ 27 kDa), L1-L2-E7-GFP (lane 2, ~ 46.5 kDa), and HSP70-L1-L2-E7-GFP (lane 3, ~ 55.5 kDa), respectively. No clear band was detected in untransfected cells as a negative control (lane 4). MW is molecular weight marker (prestained protein ladder, 10–180 kDa, Fermentas)

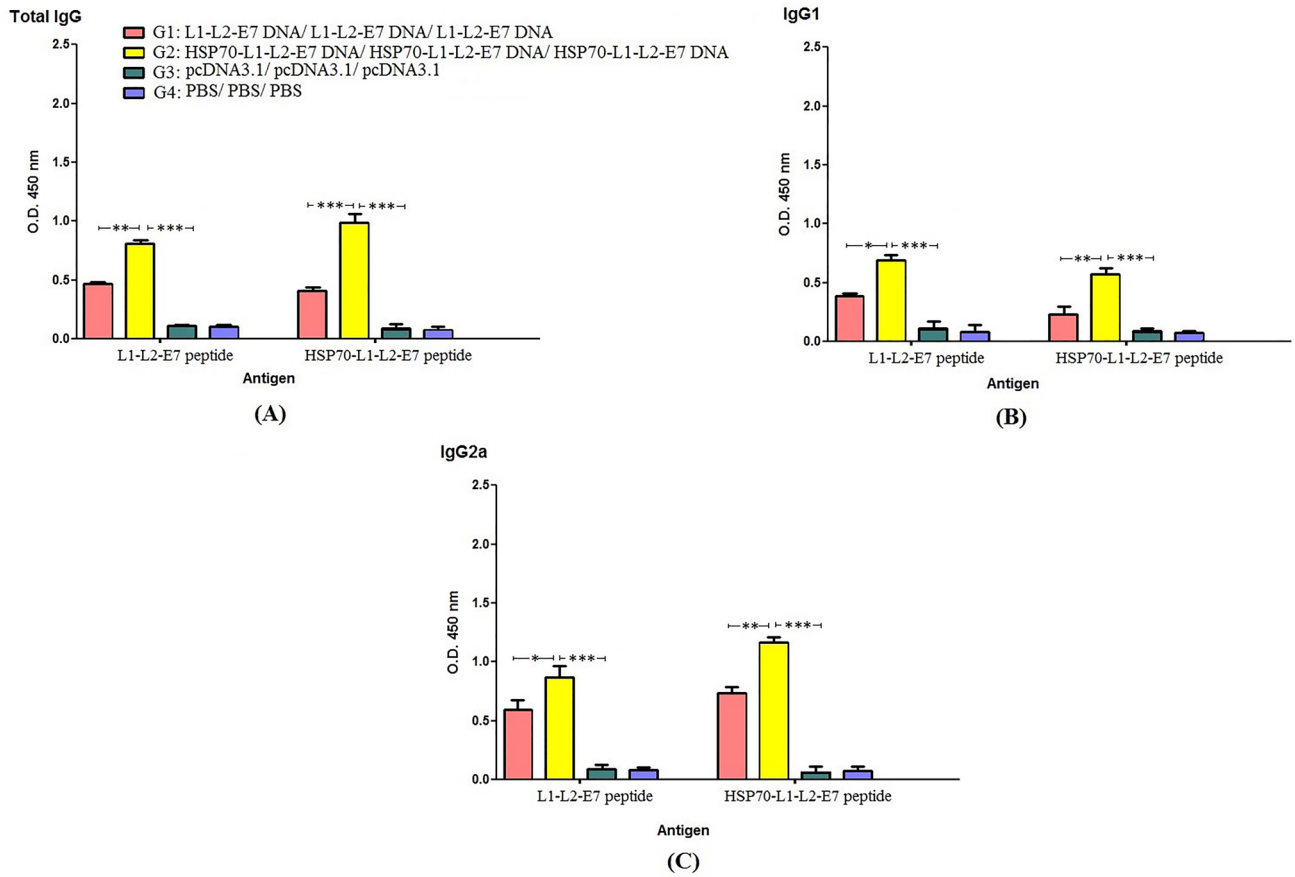

Fig. 17 Antibody responses against the L1-L2-E7 and HSP70-L1-L2-E7 peptides as an antigen in different groups: **A** total IgG, **B** IgG1, and **C** IgG2a; Mice sera were prepared from the whole blood samples of each group ($n=8$) 3 weeks after the last immunization. All analyses were performed in duplicate for each sample shown as mean absorbance at 450 nm ± SD. ***$p<0.001$; **$p<0.01$; *$p<0.05$; *ns* non-significant

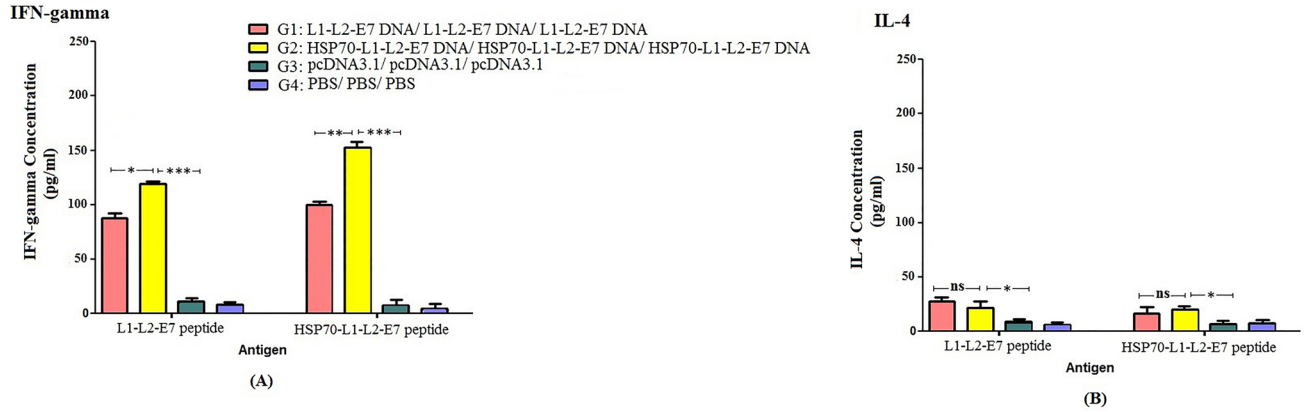

Fig. 18 The levels of IFN-γ (**A**) and IL-4 (**B**) in vaccinated groups with different formulations: The pooled splenocytes were prepared from three mice in each group ($n=3$) and re-stimulated with the L1-L2-E7 or HSP70-L1-L2-E7 peptides in vitro. The levels of cytokines were measured in the supernatant with ELISA as mean absorbance at 450 nm ± SD for each sample. All analyses were performed in duplicate for each sample. ***$p<0.001$; **$p<0.01$; *$p<0.05$; *ns* non-significant

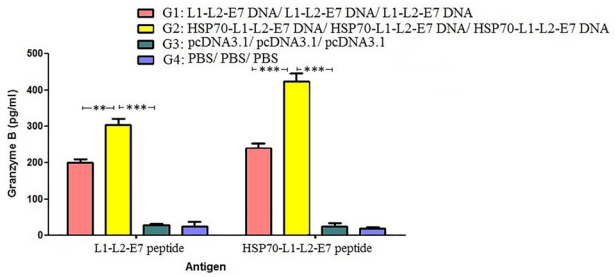

Fig. 19 Granzyme B concentration measured by ELISA using the pooled splenocytes from three mice in each group ($n=3$). All analyses were performed in triplicate for each sample. ***$p<0.001$; **$p<0.01$; *$p<0.05$; ns: non-significant

the fusion sequence of the full-length bovin papillomavirus (BPV) L1 protein and a murine E7 antigenic epitope (aa 49–57) could induce effective E7-specific antitumor immune response in mice [89].

In our study, the endotoxin-free pcDNA-L1-L2-E7 and pcDNA-HSP70-L1-L2-E7 vectors were prepared and subcutaneously injected to C57BL/6 mice. Our results showed that the HSP70-L1-L2-E7 DNA construct generated significantly total IgG, IgG2a, IgG1, and IFN-gamma against both L1-L2-E7 and HSP70-L1-L2-E7 peptides as coated antigens compared to the L1-L2-E7 DNA construct. It is important that both DNA constructs elicited higher IgG2a and IFN-gamma levels than IgG1 and IL-4 levels indicating direction of responses toward Th1 response. In addition, the secretion of Granzyme B in the group vaccinated with pcDNA-HSP70-L1-L2-E7 was higher than the group vaccinated with pcDNA-L1-L2-E7 indicating an effective CTL activity in vitro. On the other hand, the percentage of tumor-free mice in the group vaccinated with pcDNA-HSP70-L1-L2-E7 was significantly more than the group vaccinated with pcDNA-L1-L2-E7. Moreover, the tumor growth in the group vaccinated with pcDNA-HSP70-L1-L2-E7 was less than the group vaccinated with pcDNA-L1-L2-E7, but this difference was not significant. Generally, the L1-L2-E7 DNA construct was effective for inducing immune responses and antitumor effects, but the linkage of HSP70 epitopes to the L1-L2-E7 DNA construct could significantly boost its potency.

Conclusion

In summary, two multiepitope peptide vaccine candidates were designed against HPV infection using in silico studies. After their reverse translation, four eukaryotic vectors expressing the multiepitope DNA (pEGFP-L1-L2-E7, pEGFP-HSP70-L1-L2-E7, pcDNA-L1-L2-E7 and pcDNA-HSP70-L1-L2-E7) were generated and used for in vitro and in vivo studies. The data showed that both multiepitope DNA constructs were successfully expressed in mammalian cell line. Moreover, in vivo studies showed that the linkage of HSP70 epitopes to the L1-L2-E7 DNA construct could significantly increase immune responses toward Th1 response and CTL activity and induce stronger antitumor effects. However, further studies are required to evaluate other strategies such as heterologous prime/boost regimen and/or the use of chemotherapeutic agents along with vaccination. Moreover, the stability of cytokine secretion will be assessed in splenocyte and plasma in future works.

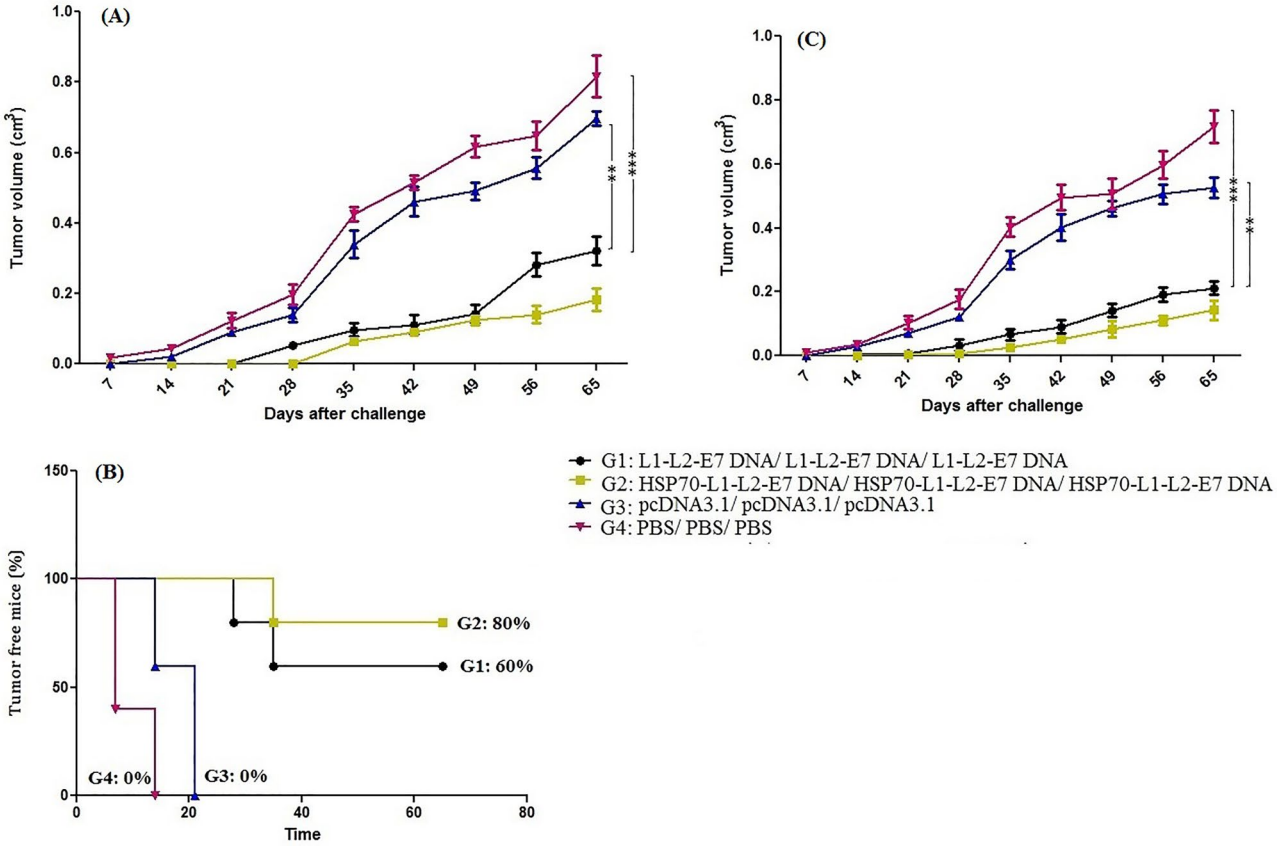

Fig. 20 Preventive study **A**, **B**: Tumor growth curve and survival percentage in different groups: The mice were challenged with 1×10^5 C3 tumor cells 3 weeks after the last immunization. Tumor volumes were measured twice a week (**A**), and the percentage of tumor-free mice (or survival rate) was evaluated in different groups (**B**); Therapeutic study (**C**): Tumor growth curve; Tumor volumes were measured twice a week. ***$p<0.001$; **$p<0.01$; *$p<0.05$; *ns* non-significant

Declarations

Conflict of interest The authors declare no conflict of interest related to this study.

References

1. Damania, B. (2016). A virological perspective on cancer. *PLoS Pathogens, 12*(2), e1005326.
2. Mesri, E. A., Feitelson, M. A., & Munger, K. (2014). Human viral oncogenesis: A cancer hallmarks analysis. *Cell Host & Microbe, 15*(3), 266–282.
3. Zapatka, M., Borozan, I., Brewer, D. S., Iskar, M., Grundhoff, A., Alawi, M., Desai, N., Sültmann, H., Moch, H., Cooper, C. S., Eils, R., Ferretti, V., & Lichter, P. (2020). The landscape of viral associations in human cancers. *Nature Genetics, 52*(3), 320–330.
4. Bravo, I. G., de Sanjosé, S., & Gottschling, M. (2010). The clinical importance of understanding the evolution of papillomaviruses. *Trends in Microbiology, 18*(10), 432–438.
5. McLaughlin-Drubin, M. E., & Munger, K. (2008). Viruses associated with human cancer. *Biochimica et Biophysica Acta (BBA)-Molecular Basis of Disease, 1782*(3), 127–150.
6. Doorbar, J., Egawa, N., Griffin, H., Kranjec, C., & Murakami, I. (2015). Human papillomavirus molecular biology and disease association. *Reviews in Medical Virology, 25*, 2–23.
7. Doorbar, J., Quint, W., Banks, L., Bravo, I. G., Stoler, M., Broker, T. R., & Stanley, M. A. (2012). The biology and life-cycle of human papillomaviruses. *Vaccine, 30*, F55–F70.
8. De Villiers, E. M. (2013). Cross-roads in the classification of papillomaviruses. *Virology, 445*(1–2), 2–10.
9. Tsakogiannis, D., Gartzonika, C., Levidiotou-Stefanou, S., & Markoulatos, P. (2017). Molecular approaches for HPV genotyping and HPV-DNA physical status. *Expert Reviews in Molecular Medicine, 19*, e1.
10. Gupta, G., Glueck, R., & Patel, P. R. (2017). HPV vaccines: Global perspectives. *Human Vaccines & Immunotherapeutics, 13*(6), 1421–1424.
11. Wang, R., Pan, W., Jin, L., Huang, W., Li, Y., Wu, D., Gao, C., Ma, D., & Liao, S. (2020). Human papillomavirus vaccine against cervical cancer: Opportunity and challenge. *Cancer Letters, 471*, 88–102.
12. Ferlay, J., Colombet, M., Soerjomataram, I., Mathers, C., Parkin, D., Piñeros, M., Znaor, A., & Bray, F. (2019). Estimating the global cancer incidence and mortality in 2018: GLOBOCAN sources and methods. *International Journal of Cancer, 144*(8), 1941–1953.
13. Dadar, M., Chakraborty, S., Dhama, K., Prasad, M., Khandia, R., Hassan, S., Munjal, A., Tiwari, R., Karthik, K., Kumar, D.,

Iqbal, H. M. N., & Chaicumpa, W. (2018). Advances in designing and developing vaccines, drugs and therapeutic approaches to counter human papilloma virus. *Frontiers in Immunology, 9*, 2478.
14. Chabeda, A., Yanez, R. J., Lamprecht, R., Meyers, A. E., Rybicki, E. P., & Hitzeroth, I. I. (2018). Therapeutic vaccines for high-risk HPV-associated diseases. *Papillomavirus Research, 5*, 46–58.
15. Harper, D. M., & DeMars, L. R. (2017). HPV vaccines-a review of the first decade. *Gynecologic Oncology, 146*(1), 196–204.
16. Joura, E. A., Giuliano, A. R., Iversen, O. E., Bouchard, C., Mao, C., & Mehlsen, J. (2015). A 9-valent HPV vaccine against infection and intraepithelial neoplasia in women. *New England Journal of Medicine, 372*(8), 711–723.
17. Kim, H. J., & Kim, H. J. (2017). Current status and future prospects for human papillomavirus vaccines. *Archives of Pharmacal Research, 40*(9), 1050–1063.
18. Yang, A., Farmer, E., Wu, T. C., & Hung, C. F. (2016). Perspectives for therapeutic HPV vaccine development. *Journal of Biomedical Science, 23*(1), 75.
19. Yang, A., Jeang, J., Cheng, K., Cheng, T., Yang, B., Wu, T. C., & Hung, C. F. (2016). Current state in the development of candidate therapeutic HPV vaccines. *Expert Review of Vaccines, 15*(8), 989–1007.
20. Namvar, A., Bolhassani, A., Javadi, G., & Noormohammadi, Z. (2019). In silico/in vivo analysis of high-risk papillomavirus L1 and L2 conserved sequences for development of cross-subtype prophylactic vaccine. *Scientific Reports, 9*(1), 1–22.
21. Bahmani, B., Amini-bayat, Z., Ranjbar, M. M., Bakhtiari, N., & Zarnani, A. H. (2021). HPV16-E7 protein T cell epitope prediction and global therapeutic peptide vaccine design based on human leukocyte antigen frequency: An in silico study. *International Journal of Peptide Research and Therapeutics, 27*, 365–378.
22. Gomez-Gutierrez, J. G., Elpek, K. G., de Oca-Luna, R. M., Shirwan, H., Zhou, H. S., & McMasters, K. M. (2007). Vaccination with an adenoviral vector expressing calreticulin-human papillomavirus 16 E7 fusion protein eradicates E7 expressing established tumors in mice. *Cancer Immunology, Immunotherapy, 56*(7), 997–1007.
23. Reinis, M., Stepanek, I., Simova, J., Bieblova, J., Pribylova, H., & Indrova, M. (2010). Induction of protective immunity against MHC class I-deficient, HPV16-associated tumours with peptide and dendritic cell-based vaccines. *International Journal of Oncology, 36*(3), 545–551.
24. Milani, A., Basirnejad, M., & Bolhassani, A. (2019). Heat-shock proteins in diagnosis and treatment: An overview of different biochemical and immunological functions. *Immunotherapy, 11*(3), 215–239.
25. Bolhassani, A., & Rafati, S. (2008). Heat-shock proteins as powerful weapons in vaccine development. *Expert Review of Vaccines, 7*(8), 1185–1199.
26. Li, Y., Subjeck, J., Yang, G., Repasky, E., & Wang, X. Y. (2006). Generation of anti-tumor immunity using mammalian heat shock protein 70 DNA vaccines for cancer immunotherapy. *Vaccine, 24*(25), 5360–5370.
27. Udono, H., Ichiyanagi, T., Mizukami, S., & Imai, T. (2009). Heat shock proteins in antigen trafficking—Implications on antigen presentation to T cells. *International Journal of Hyperthermia, 25*(8), 617–625.
28. Binder, R. J., & Srivastava, P. K. (2005). Peptides chaperoned by heat-shock proteins are a necessary and sufficient source of antigen in the cross-priming of CD8+ T cells. *Nature Immunology, 6*(6), 593–599.
29. Jiang, J., Xie, D., Zhang, W., Xiao, G., & Wen, J. (2013). Fusion of Hsp70 to Mage-a1 enhances the potency of vaccine-specific immune responses. *Journal of Translational Medicine, 11*, 300.
30. Kaliamurthi, S., Selvaraj, G., Junaid, M., Khan, A., Gu, K., & Wei, D. Q. (2018). Cancer immunoinformatics: A promising era in the development of peptide vaccines for human papillomavirus-induced cervical cancer. *Current Pharmaceutical Design, 24*(32), 3791–3817.
31. Wei, D. Q., Selvaraj, G., & Kaushik, A. C. (2018). Computational perspective on the current state of the methods and new challenges in cancer drug discovery. *Current Pharmaceutical Design, 24*(32), 3725.
32. Kaliamurthi, S., Selvaraj, G., Kaushik, A. C., Gu, K. R., & Wei, D. Q. (2018). Designing of CD8+ and CD8+-overlapped CD4+ epitope vaccine by targeting late and early proteins of human papillomavirus. *Biologics: Targets & Therapy, 12*, 107.
33. Panahi, H. A., Bolhassani, A., Javadi, G., & Noormohammadi, Z. (2018). A comprehensive in silico analysis for identification of therapeutic epitopes in HPV16, 18, 31 and 45 oncoproteins. *PLoS ONE, 13*(10), e0205933.
34. Namvar, A., Panahi, H. A., Agi, E., & Bolhassani, A. (2020). Development of HPV 16, 18, 31, 45 E5 and E7 peptides-based vaccines predicted by immunoinformatics tools. *Biotechnology Letters, 42*(3), 403–418.
35. Negahdaripour, M., Nezafat, N., Heidari, R., Erfani, N., Hajighahramani, N., Ghoshoon, M. B., Shoolian, E., Rahbar, M. R., Najafipour, S., Dehshahri, A., Morowvat, M. H., & Ghasemi, Y. (2020). Production and preliminary in vivo evaluations of a novel in silico-designed L2-based potential HPV vaccine. *Current Pharmaceutical Biotechnology, 21*(4), 316–324.
36. Bolhassani, A., & Rafati, S. (2013). Mini-chaperones: Potential immuno-stimulators in vaccine design. *Human Vaccines & Immunotherapeutics, 9*(1), 153–161.
37. Kenter, G. G., Welters, M. J., Valentijn, A. R. P., Lowik, M. J., Berends-van der Meer, D. M., & Vloon, A. P. (2009). Vaccination against HPV-16 oncoproteins for vulvar intraepithelial neoplasia. *New England Journal of Medicine, 361*(19), 1838–18347.
38. Elhassan, R. M., Alsony, N. M., Othman, K. M., Izz-Aldin, D. T., Alhaj, T. A., Ali, A. A., Abashir, L. A., Ahmed, O. H., & Hassan, M. A. (2019). Computational vaccinology approach: Designing an efficient multi-epitope peptide vaccine against *Cryptococcus neoformans var. grubii's* heat shock 70KDa protein. *BioRxiv*. https://doi.org/10.1101/534008
39. Jurtz, V., Paul, S., Andreatta, M., Marcatili, P., Peters, B., & Nielsen, M. (2017). NetMHCpan-4.0: Improved peptide–MHC class I interaction predictions integrating eluted ligand and peptide binding affinity data. *The Journal of Immunology, 199*(9), 3360–3368.
40. Jensen, K. K., Andreatta, M., Marcatili, P., Buus, S., Greenbaum, J. A., & Yan, Z. (2018). Improved methods for predicting peptide binding affinity to MHC class II molecules. *Immunology, 154*(3), 394–406.
41. Peters, B., Bulik, S., Tampe, R., Van Endert, P. M., & Holzhütter, H. G. (2003). Identifying MHC class I epitopes by predicting the TAP transport efficiency of epitope precursors. *The Journal of Immunology, 171*(4), 1741–1749.
42. Tenzer, S., Peters, B., Bulik, S., Schoor, O., Lemmel, C., Schatz, M., Kloetzel, P. M., Rammensee, H. G., Schild, H., & Holzhütter, H. G. (2005). Modeling the MHC class I pathway by combining predictions of proteasomal cleavage, TAP transport and MHC class I binding. *Cellular and Molecular Life Sciences, 62*(9), 1025–1037.
43. Calis, J. J., Maybeno, M., Greenbaum, J. A., Weiskopf, D., De Silva, A. D., Sette, A., Kesmir, C., & Peters, B. (2013). Properties of MHC class I presented peptides that enhance immunogenicity. *PLoS Computational Biology, 9*(10), e1003266.
44. Saha, S., & Raghava, G. (2006). AlgPred: Prediction of allergenic proteins and mapping of IgE epitopes. *Nucleic Acids Research, 34*(2), W202–W209.

45. Gupta, S., Kapoor, P., Chaudhary, K., Gautam, A., Kumar, R., & Raghava, G. P. (2013). In silico approach for predicting toxicity of peptides and proteins. *PLoS ONE, 8*(9), e73957.
46. Nagpal, G., Usmani, S. S., Dhanda, S. K., Kaur, H., Singh, S., Sharma, M., & Raghava, G. P. S. (2017). Computer-aided designing of immunosuppressive peptides based on IL-10 inducing potential. *Scientific Reports, 7*(1), 1–10.
47. Dhanda, S. K., Gupta, S., Vir, P., & Raghava, G. (2013). Prediction of IL-4 inducing peptides. *Clinical and Developmental Immunology, 2013*, 1–9.
48. Dhanda, S. K., Vir, P., & Raghava, G. P. (2013). Designing of interferon-γ inducing MHC class-II binders. *Biology Direct, 8*(1), 1–15.
49. Bui, H. H., Sidney, J., Dinh, K., Southwood, S., Newman, M. J., & Sette, A. (2006). Predicting population coverage of T-cell epitope-based diagnostics and vaccines. *BMC Bioinformatics, 7*(1), 1–5.
50. London, N., Raveh, B., Cohen, E., Fathi, G., & Schueler-Furman, O. (2011). Rosetta FlexPepDock web server-high resolution modeling of peptide-protein interactions. *Nucleic Acids Research, 39*(2), W249–W253.
51. Lee, H., Heo, L., Lee, M. S., & Seok, C. (2015). GalaxyPepDock: A protein–peptide docking tool based on interaction similarity and energy optimization. *Nucleic Acids Research, 43*(W1), W431–W435.
52. Jespersen, M. C., Peters, B., Nielsen, M., & Marcatili, P. (2017). BepiPred-2.0: Improving sequence-based B-cell epitope prediction using conformational epitopes. *Nucleic Acids Research, 45*(W1), W24–W29.
53. Larsen, J. E. P., Lund, O., & Nielsen, M. (2006). Improved method for predicting linear B-cell epitopes. *Immunome Research, 2*(1), 1–7.
54. Gasteiger, E., Hoogland, C., Gattiker, A., Wilkins, M. R., Appel, R. D., & Bairoch, A. (2005). *Protein identification and analysis tools on the ExPASy server* (pp. 571–607). Springer.
55. Wang, S., Li, W., Liu, S., & Xu, J. (2016). RaptorX-Property: A web server for protein structure property prediction. *Nucleic Acids Research, 44*(W1), W430–W435.
56. Yang, J., Yan, R., Roy, A., Xu, D., Poisson, J., & Zhang, Y. (2015). The I-TASSER Suite: Protein structure and function prediction. *Nature Methods, 12*(1), 7–8.
57. Lee, G. R., Heo, L., & Seok, C. (2016). Effective protein model structure refinement by loop modeling and overall relaxation. *Proteins: Structure, Function, and Bioinformatics, 84*, 293–301.
58. Lee, G. R., Heo, L., & Seok, C. (2018). Simultaneous refinement of inaccurate local regions and overall structure in the CASP12 protein model refinement experiment. *Proteins: Structure, Function, and Bioinformatics, 86*, 168–176.
59. Colovos, C., & Yeates, T. O. (1993). Verification of protein structures: Patterns of nonbonded atomic interactions. *Protein Science, 2*(9), 1511–1519.
60. Vajda, S., Yueh, C., Beglov, D., Bohnuud, T., Mottarella, S. E., Xia, B., Hall, D. R., & Kozakov, D. (2017). New additions to the C lus P ro server motivated by CAPRI. *Proteins: Structure, Function, and Bioinformatics, 85*(3), 435–444.
61. Sabroe, I., Dower, S. K., & Whyte, M. K. (2005). The role of Toll-like receptors in the regulation of neutrophil migration, activation, and apoptosis. *Clinical Infectious Diseases, 41*(7), S421–S426.
62. Tartey, S., & Takeuchi, O. (2017). Pathogen recognition and Toll-like receptor targeted therapeutics in innate immune cells. *International Reviews of Immunology, 36*(2), 57–73.
63. Feltkamp, M. C., Smits, H. L., Vierboom, M. P., Minnaar, R. P., de Jongh, B. M., Drijfhout, J. W., Schegget, J. T., Melief, C. J., & Kast, W. M. (1993). Vaccination with cytotoxic T lymphocyte epitope-containing peptide protects against a tumor induced by human papillomavirus type 16-transformed cells. *European Journal of Immunology, 23*(9), 2242–2249.
64. Guruprasad, K., Reddy, B. B., & Pandit, M. W. (1990). Correlation between stability of a protein and its dipeptide composition: A novel approach for predicting in vivo stability of a protein from its primary sequence. *Protein Engineering, Design and Selection, 4*(2), 155–161.
65. Melief, C. J., & Van Der Burg, S. H. (2008). Immunotherapy of established (pre) malignant disease by synthetic long peptide vaccines. *Nature Reviews Cancer, 8*(5), 351–360.
66. Rumfield, C. S., Roller, N., Pellom, S. T., Schlom, J., & Jochems, C. (2020). Therapeutic vaccines for HPV-associated malignancies. *ImmunoTargets and Therapy, 9*, 167–200.
67. Zong, J., Peng, Q., Wang, Q., Zhang, T., Fan, D., & Xu, X. (2009). Human HSP70 and modified HPV16 E7 fusion DNA vaccine induces enhanced specific CD8+ T cell responses and anti-tumor effects. *Oncology Reports, 22*(4), 953–961.
68. Oli, A. N., Obialor, W. O., Ifeanyichukwu, M. O., Odimegwu, D. C., Okoyeh, J. N., Emechebe, G. O., Adejumo, S. A., & Ibeanu, G. C. (2020). Immunoinformatics and vaccine development: An overview. *ImmunoTargets and Therapy, 9*, 13–30.
69. Soria-Guerra, R. E., Nieto-Gomez, R., Govea-Alonso, D. O., & Rosales-Mendoza, S. (2015). An overview of bioinformatics tools for epitope prediction: Implications on vaccine development. *Journal of Biomedical Informatics, 53*, 405–414.
70. Feltkamp, M. C., Vreugdenhil, G. R., Vierboom, M. P., Ras, E., van der Burg, S. H., Schegget, J. T., Melief, C. J. M., & Kast, W. M. (1995). Cytotoxic T lymphocytes raised against a subdominant epitope offered as a synthetic peptide eradicate human papillomavirus type 16-induced tumors. *European Journal of Immunology, 25*(9), 2638–2642.
71. Kawana, K., Yasugi, T., Kanda, T., Kino, N., Oda, K., & Okada, S. (2003). Safety and immunogenicity of a peptide containing the cross-neutralization epitope of HPV16 L2 administered nasally in healthy volunteers. *Vaccine, 21*(27–30), 4256–4260.
72. Hitzeroth, I. I., Passmore, J. A. S., Shephard, E., Stewart, D., Müller, M., Williamson, A. L., Rybicki, E. P., & Kast, W. M. (2009). Immunogenicity of an HPV-16 L2 DNA vaccine. *Vaccine, 27*(46), 6432–6434.
73. Kwak, K., Jiang, R., Jagu, S., Wang, J. W., Wang, C., Christensen, N. D., & Roden, R. B. S. (2013). Multivalent human papillomavirus l1 DNA vaccination utilizing electroporation. *PLoS ONE, 8*(3), e60507.
74. Lee, H. J., Yoon, J. K., Heo, Y., Cho, H., Cho, Y., Gwon, Y., Kim, K. C., Choi, J., Lee, J. S., Oh, Y. K., & Kim, Y. B. (2015). Therapeutic potential of an AcHERV-HPV L1 DNA vaccine. *Journal of Microbiology, 53*(6), 415–420.
75. McGrath, M., de Villiers, G. K., Shephard, E., Hitzeroth, I. I., & Rybicki, E. P. (2013). Development of human papillomavirus chimaeric L1/L2 candidate vaccines. *Archives of Virology, 158*(10), 2079–2088.
76. Wu, W. H., Alkutkar, T., Karanam, B., Roden, R. B., Ketner, G., & Ibeanu, O. A. (2015). Capsid display of a conserved human papillomavirus L2 peptide in the adenovirus 5 hexon protein: A candidate prophylactic hpv vaccine approach. *Virology Journal, 12*(1), 140.
77. Sabah, S. N., Gazi, M. A., Sthity, R. A., Husain, A. B., Quyyum, S. A., Rahman, M., & Islam, M. R. (2018). Designing of epitope-focused vaccine by targeting E6 and E7 conserved protein sequences: An immuno-informatics approach in human papillomavirus 58 isolates. *Interdisciplinary Sciences: Computational Life Sciences, 10*(2), 251–260.
78. Tsang, K. Y., Fantini, M., Fernando, R. I., Palena, C., David, J. M., Hodge, J. W., Gabitzsch, E. S., Jones, F. R., & Schlom, J. (2017). Identification and characterization of enhancer agonist human cytotoxic T-cell epitopes of the human papillomavirus type 16 (HPV16) E6/E7. *Vaccine, 35*(19), 2605–2611.

79. Chen, C. H., Wang, T. L., Hung, C. F., Yang, Y., Young, R. A., Pardoll, D. M., & Wu, T. C. (2000). Enhancement of DNA vaccine potency by linkage of antigen gene to an HSP70 gene. *Cancer Research, 60*(4), 1035–1042.
80. Zong, J., Wang, C., Wang, Q., Peng, Q., Xu, Y., Xie, X., & Xu, X. (2013). HSP70 and modified HPV 16 E7 fusion gene without the addition of a signal peptide gene sequence as a candidate therapeutic tumor vaccine. *Oncology Reports, 30*(6), 3020–3026.
81. Matsui, H., Hazama, S., Tamada, K., Udaka, K., Irie, A., Nishimura, Y., Miyakawa, T., Doi, S., Nakajima, M., Kanekiyo, S., Tokumitsu, Y., Shindo, Y., Tomochika, S., Yoshida, S., Iida, M., Suzuki, N., Takeda, S., Yamamoto, S., Yoshino, S., … Nagano, H. (2019). Identification of a promiscuous epitope peptide derived from HSP70. *Journal of Immunotherapy, 42*(7), 244.
82. Day, P. M., Thompson, C. D., Lowy, D. R., & Schiller, J. T. (2017). Interferon gamma prevents infectious entry of human papillomavirus 16 via an L2-dependent mechanism. *Journal of Virology, 91*(10), 1–10.
83. Theodoropoulos, G. E., Saridakis, V., Karantanos, T., Michalopoulos, N. V., Zagouri, F., Kontogianni, P., Lymperi, M., Gazouli, M., & Zografos, G. C. (2012). Toll-like receptors gene polymorphisms may confer increased susceptibility to breast cancer development. *The Breast, 21*(4), 534–538.
84. Dabbagh, K., & Lewis, D. B. (2003). Toll-like receptors and T-helper-1/T-helper-2 responses. *Current Opinion in Infectious Diseases, 16*(3), 199–204.
85. Yang, X., Cheng, Y., & Li, C. (2017). The role of TLRs in cervical cancer with HPV infection: A review. *Signal Transduction and Targeted Therapy, 2*(1), 1–10.
86. El-Omar, E., Ng, M., & Hold, G. (2008). Polymorphisms in toll-like receptor genes and risk of cancer. *Oncogene, 27*(2), 244–252.
87. de Matos, L. G., Cândido, E. B., Vidigal, P. V., Bordoni, P. H., Lamaita, R. M., Carneiro, M. M., & da Silva-Filho, A. L. (2017). Association between Toll-like receptor and tumor necrosis factor immunological pathways in uterine cervical neoplasms. *Tumori Journal, 103*(1), 81–86.
88. Choi, Y. J., Hur, S. Y., Kim, T. J., Hong, S. R., Lee, J. K., Cho, C. H., Park, K. S., Woo, J. W., Sung, Y. C., Suh, Y. S., & Park, J. S. (2020). A phase II, prospective, randomized, multicenter, open-label study of GX-188E, an HPV DNA vaccine, in patients with cervical intraepithelial neoplasia 3. *Clinical Cancer Research, 26*, 1616–1623.
89. Yang, A., Peng, S., Farmer, E., Zeng, Q., Cheng, M. A., Pang, X., Wu, T. C., & Hung, C. F. (2017). Enhancing antitumor immunogenicity of HPV16-E7 DNA vaccine by fusing DNA encoding E7-antigenic peptide to DNA encoding capsid protein L1 of Bovine papillomavirus. *Cell & Bioscience, 7*, 46.